AD_____

Award Number: DAMD17-01-1-0108

TITLE: Tumor Oxygen Dynamics as a Prognostic Indicator of Effective Antiangiogenic Therapy

PRINCIPAL INVESTIGATOR: Dawen Zhao, M.D., Ph.D.
Ralph P. Mason, Ph.D.

CONTRACTING ORGANIZATION: The University of Texas Southwestern Medical Center at Dallas
Dallas, Texas 75390-9105

REPORT DATE: May 2002

TYPE OF REPORT: Annual Summary

PREPARED FOR: U.S. Army Medical Research and Materiel Command
Fort Detrick, Maryland 21702-5012

REPORT DOCUMENTATION PAGE

Form Approved
OMB No. 074-0188

1. AGENCY USE ONLY (Leave blank)	2. REPORT DATE	3. REPORT TYPE AND DATES COVERED
	May 2002	Annual Summary (1 May 01 - 30 Apr 02)

4. TITLE AND SUBTITLE
Tumor Oxygen Dynamics as a Prognostic Indicator of Effective Antiangiogenic Therapy

5. FUNDING NUMBERS
DAMD17-01-1-0108

6. AUTHOR(S)
Dawen Zhao, M.D., Ph.D.
Ralph P. Mason, Ph.D.

7. PERFORMING ORGANIZATION NAME(S) AND ADDRESS(ES)
The University of Texas Southwestern
Medical Center at Dallas
Dallas, Texas 75390-9105
E-Mail: dawen.zhao@UTSouthwestern.edu

8. PERFORMING ORGANIZATION REPORT NUMBER

9. SPONSORING / MONITORING AGENCY NAME(S) AND ADDRESS(ES)
U.S. Army Medical Research and Materiel Command
Fort Detrick, Maryland 21702-5012

10. SPONSORING / MONITORING AGENCY REPORT NUMBER

11. SUPPLEMENTARY NOTES

12a. DISTRIBUTION / AVAILABILITY STATEMENT
Approved for Public Release; Distribution Unlimited

12b. DISTRIBUTION CODE

13. ABSTRACT *(Maximum 200 Words)*

Tumor survival, growth and metastasis depend critically on the development of new blood vessels: so called angiogenesis. One major goal of this project is to fully understand and precisely assess the dynamic changes in blood perfusion and oxygenation, both during nomal growth and following anti-angiogenic therapy in several prostate tumors with differential characteristics, so that we may predict response and optimize the therapy. Combined *BOLD* (Blood oxygen level dependent) MRI with our *FREDOM* (Fluorocarbon Relaxometry using Echo planar imaging for Dynamic Oxygen Mapping) MR, our results showed that significantly better oxygenation was found in the well differentiated and slower growing H and HI tumors, compared with anaplastic or metastatic, faster growing AT1 and MAT-Lu tumors. These MRI data has been compared and validated by cellular and molecular biology. Compared with the level of hypoxia (pimonidazole) and vasculature (CD31) in H and HI tumors, the AT1 tumors have a higher labelling index for pimonidazole and lower vascular density. An interesting finding is that expression of HIF-1α and VEGF was found in relatively well differentiated and oxygenated H and HI tumors, which did not overlap with hypoxic regions recognized by pimonidazole. However, there was no expression in the AT1 tumors.

14. Subject Terms (keywords previously assigned to proposal abstract or terms which apply to this award)	15. NUMBER OF PAGES
Magnetic resonance imaging (MRI), pO_2, hypoxic maker, VEGF, Anti-angiogenic therapy	63
	16. PRICE CODE

17. SECURITY CLASSIFICATION OF REPORT	18. SECURITY CLASSIFICATION OF THIS PAGE	19. SECURITY CLASSIFICATION OF ABSTRACT	20. LIMITATION OF ABSTRACT
Unclassified	Unclassified	Unclassified	Unlimited

Table of Contents

Background:

The diagnosis and treatment of cancers are beginning to be influenced by new ideas and discoveries emerging from the field of angiogenesis. Dr. Folkman noted that microvascular endothelial cell (MEC) activity controls proliferation and aggressiveness of tumors, and the absence of angiogenesis leads to a lack of tumor cell proliferation (1). Folkman and his colleagues hypothesized that since tumors require a blood supply to grow, inhibiting the growth of new blood vessels, i.e., antiangiogenesis, should prevent growth and metastasis of the primary tumor (2). Traditional methods for detection of therapeutic response generally rely on a gross decrease in tumor size. Although these methods are useful for assessing response at the end of treatment, little information is available early in the course of treatment. MRI has the ability to detect treatment-induced changes occurring within the tumor prior to a decrease in tumor size. One major goal of this project is to fully understand and precisely assess the dynamic changes in blood perfusion and oxygenation, both during normal growth and following anti-angiogenic therapy in several prostate tumors with differential characteristics, so that we may predict response and optimize the therapy.

Body:

Initial preparation for research in Year 1 started with animal handling, tumor implantation, and perfusion. I received accreditation from the Institutional Animal Care and Research Advisory committee Board (IACRAC) to proceed with my animal studies. I successfully implanted an orthotopic prostate tumor by injecting minced tumor tissues into rat prostate gland.

I am receiving training and becoming proficient in state of the art MRI techniques. *FREDOM* (Fluorocarbon Relaxometry using Echo planar imaging for Dynamic Oxygen Mapping) with hexafluorobenzene, as a reporter molecule, exploits the exceptional response of the ^{19}F NMR spin-lattice relaxation rate to changes in oxygen tension. Echo planar MRI provides measurements with high temporal resolution (~8 mins) and a spatial resolution (>100 × 4 mm^3 voxels). This facilitates sequential reproducible measurements (±1-2 torr) (3, 4). Blood oxygen level dependent (BOLD) MRI is a totally non-invasive approach to provide a qualitative evaluation of blood oxygen level in tumor (5). The large paramagnetic susceptibility of deoxyhemoglobin produces large magnetic field gradients between blood vessels and surrounding tissues. Dynamic contrast enhanced (DCE) MRI based on the transport properties of gadolinium-DTPA (Gd-DTPA) has been used as a method in the clinic to provide an indication of tumor vasculature and perfusion by imaging the uptake, or leakage, of contrast agent into tumor interstitial space (6, 7). I am applying these MR techniques to extensively study oxygenation and vasculature in prostate tumors. **Based on these results two peer reviewed papers (one in press and one submitted) and four abstracts have been accomplished (8-13).** Our results obtained using *FREDOM* showed better tissue oxygen tension in well differentiated and slower growing Dunning R3327 prostate rat H and HI tumors, compared with anaplastic or metastatic, faster growing AT1 and MAT-Lu tumors. Most interestingly, by using *FREDOM* to track oxygen dynamics in specific tumor regions, we found that most hypoxic regions in the H and HI tumor responded to oxygen or carbogen inhalation to become well oxygenated, while those in the AT1 and MAT-Lu tumors showed little response to respiratory intervention (See Appended publications for details). Results of BOLD and DCE MRI, providing information about qualitative vascular oxygenation and perfusion, also showed that the H tumors are better oxygenated and perfused than the AT1 tumors [Fig. 1].

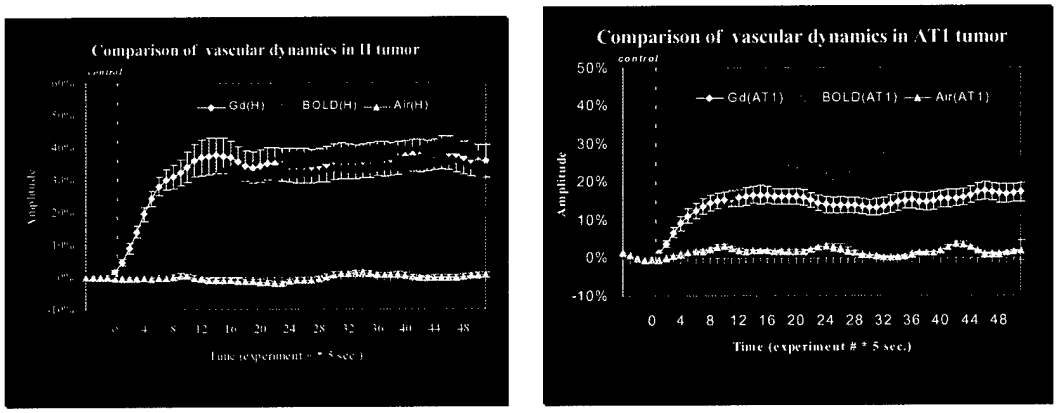

Fig. 1 Tumor vascular dynamics.
Variation in mean ^{1}H MR signal intensity in response to breathing oxygen (*BOLD*) or Magnevist™ infusion (Gd) for groups of H (a) and AT1 (b) tumors. In each case, the *BOLD* response is delayed by ~ 40 s compared with Magnevist. Both *BOLD* and Magnevist effects were greater in H tumors than AT1. The light blue trace shows stability of signal in the absence of intervention. Lines indicate mean ± se.

I have also performed extensive studies on tumor blood vessels, perfusion, and hypoxia in the Dunning prostate tumors. Immunohistochemical studies of tumor hypoxia and vasculature using hypoxic marker pimonidazole and endothelium marker CD31 showed that a higher labelling index of pimonidazole and lower vasular density in the AT1 than the H and HI tumors [Fig. 2]. Comparable results by cellular and molecular biology support our MRI findings. An interesting finding is that expression of HIF-1α was found in relatively well differentiated and oxygenated H and HI tumors [Fig. 3], which did not overlap with hypoxic regions recognized by pimonidazole. However, there was no expression in the poorly oxygenated AT1 tumors.

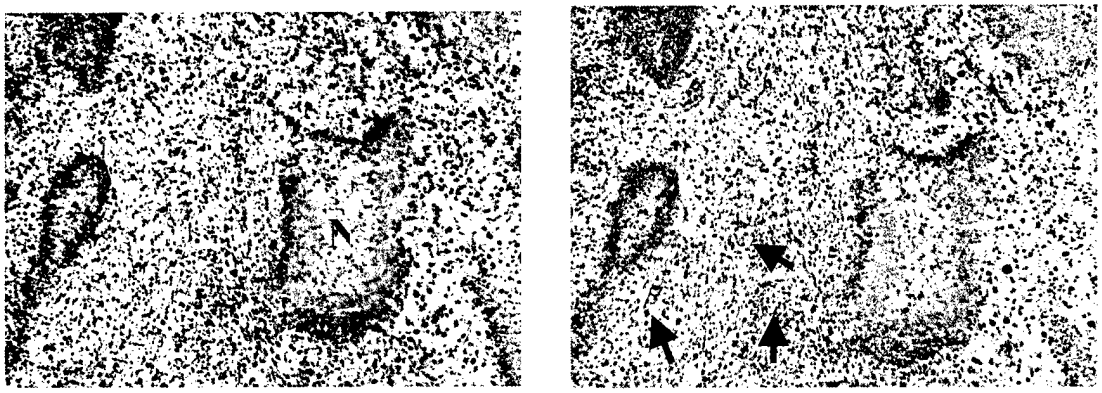

Fig. 2 Comparison of pimonidazole, CD31 in a representative AT1 tumor. Typical distribution of hypoxia in the AT1, recognized as positive staining for pimonidazole (brown, top left), was observed at some distance from blood vessels stained for CD31 (arrow, top right) and located adjacent to necrotic regions (N).

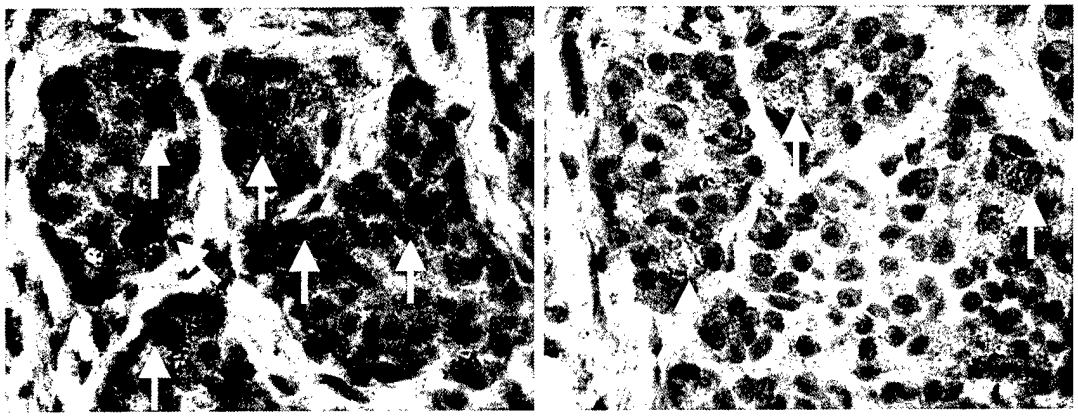

Fig. 3 HIF-1α (arrows, left) detected in both cytoplasm and nucleus of the better oxygenated H tumor cells, was co-localized with VEGF positive staining (arrows, right) in a consecutive 6 μm section.

Problems in accomplishing the tasks

I shifted the MR evaluation of tumor angiogenesis in response to antiangiogenic therapy to Year 2, which was proposed to pursue in the second half of the Year 1. This adjustment was due to unexpected breakdown of the 4.7 T magnet in Rogers NMR center. The problem has recently been fixed and a new Varian Unity INOVA system is equipped. Also, the spectrometer will be upgraded with more powerful gradients during summer '02. Preliminary data obtained using the new system has shown consistent results with our previous ones.

Key Research Accomplishments

- **Learned animal tumor implantation**
  Implantation of Dunning prostate R3327 rat tumor
- **Learned and becoming proficient in the state of art NMR techniques**
  a. *FREDOM* (Fluorocarbon Relaxometry using Echo planar imaging for Dynamic Oxygen Mapping)
  b. *BOLD* (blood oxygen level dependent) MRI
  c. Dynamic contrast enhanced (DCE) MRI
  d. Learned operating system of new Varian MR
- **Assessment of tumor perfusion and oxygenation during normal growth of prostate tumors by MR approaches**
  a. Better tissue oxygen tension in Dunning R3327 prostate rat H and HI tumors, compared with AT1 and MAT-Lu tumors.
  b. Most hypoxic regions in the H and HI tumor responded to oxygen or carbogen inhalation to become well oxygenated, while those in the AT1 and MAT-Lu tumors showed little response to respiratory intervention.
  c. Results of BOLD and DCE MRI, providing information about qualitative vascular oxygenation and perfusion.
- **Correlation of MR findings with biological studies**
  a. Immunohistochemical studies of tumor hypoxia and vasculature using hypoxic marker pimonidazole and endothelium marker CD31 supported our MR findings.
  b. Expression of HIF-1α and VEGF was found in the H and HI tumors, which did not overlap with hypoxic regions recognized by pimonidazole. However, there was no expression in the AT1 tumors.

c. Administration of perfusion marker Hoechst dye 33342 showed a good correlation between perfused vessels and total vessels (CD31) in the HI tumors.
d. RT-PCR showing no significant difference in HIF-1α gene expression between H and AT1 tumor.

Reportable Outcomes

Reportable outcomes that have resulted from this research endeavor include:

Peer Reviewed Publications:

1. **Zhao, D.**, Constantinescu, A., Hahn, E. W., and Mason, R. P. Differential oxygen dynamics in the two Dunning prostate R3327 rat tumor sublines (MAT-Lu and HI) with respect to growth and respiratory challenge. *Int. J. Radiat. Oncol. Biol. Phys.* in the press 2002.
2. **Zhao, D.**, Constantinescu, A., Hahn, E. W., and Mason, R. P. Correlation of tumor oxygen dynamics with radiation response of the Dunning prostate R3327-HI tumors. *Radiat. Res.* Submitted 2002.

Abstracts (Published Conference Proceedings):

1. **Zhao, D.**, Jiang, L., Constantinescu, A., Hahn, E.W., and Mason, R.P. In vivo MRI monitoring of prostate tumor vasculature and oxygen dynamics. *AACR New Discoveries in Prostate Cancer Biology and Treatment*, # B-56, Naples, FL, Dec 2001.
2. **Zhao, D.**, Ran, S., Constantinescu, A., Hahn, E.W., and Mason, R.P. In vivo MRI monitoring of tumor oxygen dynamics and correlation with histological findings. *4th International Symposium on Anti-Angiogenic Agents*, Dallas, TX, Jan 2002.
3. **Zhao, D.**, Hahn, E.W., Constantinescu, A., Ran, S., and Mason, R.P. Comparison of hypoxia and microvascular density in the slow growing well differentiated H vs. the faster growing anaplastic AT1 Dunning prostate R3327 rat tumor. *49th Radiat. Res. Soc.* # P10-87, Reno, NV, Apr 2002.
4. **Zhao, D.**, Constantinescu, A., Chang, K., Gall, K., Hahn, E.W., and Mason, R.P. Measurement of tumor oxygen dynamics correctly predicts beneficial adjuvant intervention for radiotherapy in Dunning prostate R3327-HI tumors. *10th ISMRM*, #2149, Honolulu, Hawaii, May 2002.

Conclusion:

Results reported here were successful in terms of the outlined tasks cited in the original proposed statement of work. Six publications have been achieved during the Year 1. I have started therapeutic experiments using antiangiogenic agent thalidomide as well as MR studies following the treatment. I expect MR studies will facilitate us to fully understand and precisely assess the dynamic changes in blood perfusion and oxygenation following anti-angiogenic therapy in prostate tumors, so that we may predict response and optimize the therapy.

References:

1. Folkman, J. Tumor angiogenesis, Adv. Cancer Res. *19:* 331-58, 1974.
2. Folkman, J. Anti-angiogenesis: new concept for therapy of solid tumors, Ann. Surg. *175:* 409-416, 1972.
3. Mason, R. P., Rodbumrung, W., and Antich, P. P. Hexafluorobenzene: a sensitive ^{19}F NMR indicator of tumor oxygenation, NMR Biomed. *9:* 125-134, 1996.
4. Hunjan, S., **Zhao, D.**, Constantinescu, A., Hahn, E. W., Antich, P. P., and Mason, R. P. Tumor Oximetry: demonstration of an enhanced dynamic mapping procedure using fluorine-19 echo planar

magnetic resonance imaging in the Dunning prostate R3327-AT1 rat tumor, Int. J. Radiat. Oncol. Biol. Phys. *49:* 1097-1108, 2001.

5. Taylor, J. S. and Reddick, W. E. Evolution from empirical dynamic contrast-enhanced magnetic resonance imaging to pharmacokinetic MRI, Adv. Drug Delivery Reviews. *41:* 91-110, 2000.
6. Evelhoch, J. L., Gillies, R. J., Karczmar, G. S., Koutcher, J. A., Maxwell, R. J., Nalcioglu, O., Raghunand, N., Ronen, S. M., Ross, B. D., and Swartz, H. M. Application of magnetic resonance in model systems: cancer therapeutics, Neoplasia. *152:* 152-65, 2000.
7. Robinson, S. P., Howe, F. A., Rodrigues, L. M., Stubbs, M., and Griffiths, J. R. Magnetic resonance imaging techniques for monitoring changes in tumor oxygenation and blood flow, Semin. Radiat. Oncol. *8:* 198-207, 1998.
8. **Zhao, D.**, Constantinescu, A., Hahn, E. W., and Mason, R. P. Differential oxygen dynamics in the two Dunning prostate R3327 rat tumor sublines (MAT-Lu and HI) with respect to growth and respiratory challenge. *Int. J. Radiat. Oncol. Biol. Phys.* in the press 2002.
9. **Zhao, D.**, Constantinescu, A., Hahn, E. W., and Mason, R. P. Correlation of tumor oxygen dynamics with radiation response of the Dunning prostate R3327-HI tumors. *Radiat. Res.* Submitted 2002.
10. **Zhao, D.**, Jiang, L., Constantinescu, A., Hahn, E.W., and Mason, R.P. In vivo MRI monitoring of prostate tumor vasculature and oxygen dynamics. *AACR New Discoveries in Prostate Cancer Biology and Treatment*, # B-56, Naples, FL, Dec 2001.
11. **Zhao, D.**, Ran, S., Constantinescu, A., Hahn, E.W., and Mason, R.P. In vivo MRI monitoring of tumor oxygen dynamics and correlation with histological findings. *4th International Symposium on Anti-Angiogenic Agents*, Dallas, TX, Jan 2002.
12. **Zhao, D.**, Hahn, E.W., Constantinescu, A., Ran, S., and Mason, R.P. Comparison of hypoxia and microvascular density in the slow growing well differentiated H vs. the faster growing anaplastic AT1 Dunning prostate R3327 rat tumor. *49th Radiat. Res. Soc.* # P10-87, Reno, NV, Apr 2002.
13. **Zhao, D.**, Constantinescu, A., Chang, K., Gall, K., Hahn, E.W., and Mason, R.P. Measurement of tumor oxygen dynamics correctly predicts beneficial adjuvant intervention for radiotherapy in Dunning prostate R3327-HI tumors. *10th ISMRM*, #2149, Honolulu, Hawaii, May 2002.

Appendices

ELSEVIER

PII S0360-3016(02)02822-5

BIOLOGY CONTRIBUTION

DIFFERENTIAL OXYGEN DYNAMICS IN TWO DIVERSE DUNNING PROSTATE R3327 RAT TUMOR SUBLINES (MAT-Lu AND HI) WITH RESPECT TO GROWTH AND RESPIRATORY CHALLENGE

DAWEN ZHAO, M.D., PH.D., ANCA CONSTANTINESCU, PH.D., ERIC W. HAHN, PH.D., AND RALPH P. MASON, PH.D.

Department of Radiology, Advanced Radiological Sciences, University of Texas Southwestern Medical Center, Dallas, TX

Purpose: Since hypoxia may influence tumor response to therapy and prognosis, we have compared oxygenation of tumors known to exhibit differential growth rate and tissue differentiation.
Methods and Materials: Regional tumor oxygen tension was measured using ^{19}F nuclear magnetic resonance echo planar imaging relaxometry of hexafluorobenzene, which provided dynamic maps with respect to respiratory intervention. Investigations used two Dunning prostate R3327 rat tumor sublines: the fast growing, highly metastatic MAT-Lu and the moderately well-differentiated, slower growing HI.
Results: Both sublines showed significantly higher oxygen tension in smaller tumors (<2 cm^3) than in larger tumors (>3.5 cm^3). Pooled data showed that MAT-Lu tumors exhibited greater hypoxia compared with the size-matched HI tumors ($p < 0.0001$). Respiratory challenge (oxygen or carbogen) produced significant increases in mean pO_2 for tumors of both sublines ($p < 0.0001$). However, initially hypoxic regions displayed very different behavior in each subline: those in the HI tumors responded rapidly with significant elevation in pO_2, while those in the MAT-Lu tumors showed little response to respiratory intervention.
Conclusions: These results concur with hypotheses that hypoxia is related to tumor growth rate and degree of differentiation. Under baseline conditions, the differences were subtle. However, response to respiratory intervention revealed highly significant differences, which, if held valid in the clinic, could have prognostic value.
© 2002 Elsevier Science Inc.

Oxygen, Magnetic resonance imaging, Prostate tumor, Hypoxia, Differentiation.

INTRODUCTION

Hypoxia in solid tumors has been widely recognized as a potent factor, which leads to resistance to radiotherapy (1, 2), photodynamic therapy (3), and some anticancer drugs (1). Further, recent studies suggest that tumor hypoxia might also be associated with malignant progression in solid tumors (4, 5). Therefore, accurate measurement of tumor oxygenation, assessment of levels of hypoxia in individual tumors, and the development of effective methods to reduce the hypoxic fraction may well contribute to therapeutic outcome. Given the importance of oxygen, many techniques for monitoring oxygen tension (pO_2) have been developed (6). While each method has specific attributes, many are highly invasive, and impractical for longitudinal studies of specific regions of interest. Nuclear magnetic resonance (NMR) is entirely noninvasive: ^{31}P NMR provides an indirect estimate of hypoxia based on phosphorylation potential (7), but the measured metabolic hypoxia occurs at a higher pO_2 than radiobiological hypoxia, and some studies have shown a lack of correlation between high-energy phosphate metabolites and pO_2 (8). Blood Oxygen Level Dependent (BOLD) contrast proton magnetic resonance imaging (MRI) provides an indication of tumor vascular oxygenation, and heterogeneity, in response to intervention, but the method does not provide pO_2 values and interpretation may be complicated by flow, hence, the concept FLOOD (FLOw and Oxygenation Dependent contrast) (9).

We recently demonstrated the feasibility of measuring tumor oxygenation based on ^{19}F NMR echo planar imaging (EPI) after direct intratumoral injection (i.t.) of hexafluorobenzene (HFB) (10, 11), for which we have chosen the

Reprint requests to: Ralph P. Mason, Ph.D., C. Chem., Department of Radiology, U.T. Southwestern Medical Center, 5323 Harry Hines Blvd., Dallas, TX 75390-9058. Tel: (214) 648-8926; Fax: (214) 648-2991; E-mail: Ralph.Mason@UTSouthwestern.edu

Presented in part at the Forty-seventh Annual Meeting of the Radiation Research Society, Albuquerque, NM, April 2000.

This work was supported in part by NIH RO1 CA79515, the American Cancer Society (RPG-97-116-010CCE), and a postdoctoral fellowship from the DOD Prostate Cancer Initiative (DAMD 170110108) (DZ). NMR experiments were performed at the Mary Nell and Ralph B. Rogers MR Center, an NIH BRTP Facility P41-RR02584.

Acknowledgments—We are grateful to Drs. Peter Antich and Peter Peschke for collegial support and Drs. Sophia Ran and Mark Jeffrey for technical assistance.

Received Nov 16, 2001, and in revised form Mar 6, 2002. Accepted for publication Mar 8, 2002.

acronym *FREDOM* (Fluorocarbon Relaxometry using Echo planar imaging for Dynamic Oxygen Mapping). This technique allows us to assess baseline pO_2 at multiple locations within a tumor, and to follow dynamic changes in response to interventions. Hexafluorobenzene has many strengths as a reporter molecule; it is readily available, cheap, and nontoxic. In terms of NMR, the sixfold symmetry provides a single ^{19}F signal offering maximum signal to noise, and the long relaxation times (T1 and T2) facilitate echo planar imaging. The spin lattice relaxation rate R1 is very sensitive to changes in pO_2, but shows minimal response to variations in temperature. HFB is readily administered through a fine needle and remains at the site of administration for several hours ($t_{1/2}$ typically 600 min) (12).

We have now applied the technique to investigate oxygen distribution and dynamics in two rat prostate tumor sublines exhibiting diverse characteristics. Although the baseline oxygenation of the moderately well-differentiated subline (HI) has been investigated previously using electrodes (13), we are unaware of previous investigations of oxygenation in the highly metastatic and poorly differentiated MAT-Lu subline. Furthermore, comparison of response to interventions, here respiratory challenge with oxygen and carbogen, is now established using a single technique for comparison of both sublines.

METHODS AND MATERIALS

Experiments were approved by the Institutional Animal Care and Research Advisory Committee.

Tumor model

Two sublines of the Dunning prostate R3327 adenocarcinoma were selected: HI, a moderately well-differentiated, slower growing, hormone-insensitive, nonmetastatic subline with tumor volume doubling time (VDT) of 9 days (14), and MAT-Lu, a highly metastatic, poorly differentiated subline with VDT of 2.7 days (15). Tumors were implanted in a skin pedicle surgically created on the foreback of adult male Copenhagen-2331 rats (~250 g, Harlan), as described in detail elsewhere (16). Tumors were allowed to grow and investigated by MRI when about 1.5 cm^3 or when greater than 3.5 cm^3 volume (~15 mm or greater than 20 mm diameter). In total, we investigated seven HI tumors including three small (size range 1.1–1.7 cm^3) and four large (range 3.5–4.6 cm^3), and eight MAT-Lu tumors including four small (range 1.2–1.9 cm^3) and four large tumors (range 3.7–5.0 cm^3). In preparation for MRI, each rat was given 200 μL ketamine hydrochloride (100 mg/mL, Aveco, Fort Dodge, IA) as a relaxant (i.m.). The rats were maintained under general gaseous anesthesia with FO_2 = 33% (fraction of inhaled O_2: 0.3 dm^3/min O_2, 0.6 dm^3/min N_2O, and 0.5% methoxyflurane [MF]; Pittman-Moore, Washington Crossing, NJ) using a small animal anesthesia unit. Hexafluorobenzene (45 μL, Lancaster, Gainesville, FL), was deoxygenated by bubbling nitrogen for 5 min before use, and injected directly into the tumors using a Hamilton syringe (Reno, NV) with a custom-made fine sharp needle (32G). The HFB was deliberately deposited in both the central and peripheral regions of the tumors to ensure that the interrogated regions would be representative of the whole tumor and for comparison with the oxygen electrode method. Generally, HFB was administered along two or three tracks in the form of a fan in a single central plane of the tumor sagittal to the rat's body. The needle was inserted manually to penetrate across the whole tumor and withdrawn ~1 mm to reduce pressure, and 3 μL HFB was deposited. The needle was repeatedly withdrawn a further 2–3 mm and additional HFB was deposited. Each rat was placed on its side in a cradle with a thermal blanket to maintain body temperature. A fiber optic probe was placed in the rectum to monitor core temperature.

Assessment of HFB distribution

Magnetic resonance experiments were performed using an Omega CSI 4.7 horizontal bore magnet system with actively shielded gradients (Bruker Instrument Inc., Fremont, CA). A tunable ($^1H/^{19}F$) single-turn solenoid coil (2 or 3 cm in diameter matched to the tumor size) was placed around the tumor-bearing pedicle. Shimming was performed on the ^1H signal (200.11 MHz) of the tissue water to a typical linewidth of 115 Hz. Proton images were obtained for anatomic reference using a three-dimensional (3D) spin-echo sequence. Imaging parameters were: repetition time (TR) = 150 ms; echo time (TE) = 8 ms; pulse width $\pi/2$ = 32 μs with 128 × 64 × 8 data points over a 40 mm field of view in plane, and 40 mm thickness, providing 312 μm × 624 μm × 5 mm digital resolution. Two transients were acquired at each phase-encoding increment, giving a total acquisition time of 2.5 min. The coil was retuned in place to 188.27 MHz, and corresponding ^{19}F MR images were obtained as a 3D data set with 128 × 32 × 8 data points and gradients compensated for the difference in gyromagnetic ratios, yielding 312 μm × 1.2 mm × 5 mm resolution. For ^{19}F MRI, a driven-equilibrium sequence was applied with TR = 150 ms, TE = 8 ms, $\pi/2$ = 50 μs excitation pulse and 16 transients at each increment, giving a total accumulation time of 10 min for the 3D data set. Driven equilibrium both enhanced the efficiency of data acquisition and provided signal corresponding primarily to spin density. Data were processed using sine-bell apodization and zero filling in the first phase-encode dimension.

Tumor oximetry

FREDOM. Following conventional MR imaging, tumor oxygenation was estimated on the basis of ^{19}F pulse burst saturation recovery (PBSR) EPI relaxometry of the HFB, as described previously (11). The *ARDVARC* (Alternated R1 Delays with Variable Acquisitions to Reduce Clearance effects) data acquisition protocol was applied to optimize data quality. This approach provided pO_2 maps with 1.25 mm in-plane voxel resolution in 8 min with typically ~50–150 individual pO_2 measurements (voxels per tumor). The spin-lattice relaxation rate [R1 (s^{-1}) = 1/T1] was estimated

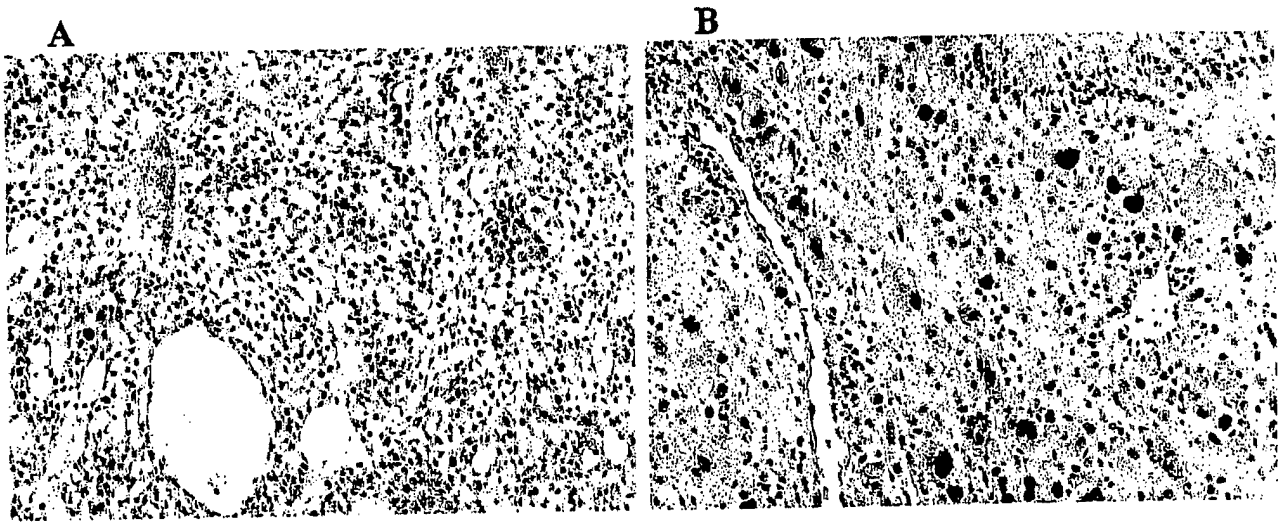

Fig. 1. Immunohistochemical comparison of HI and MAT-Lu tumors. PCNA is detected in nucleus of tumor cells. A representative HI tumor (A) with labeling index 15%, and a MAT-Lu (B) showing 40% positive index. Original magnification ×100.

on a voxel-by-voxel basis using a three-parameter monoexponential function, and pO_2 was estimated using the relationship pO_2 (mm Hg) = (R1−0.0835)/0.001876 (11). Three consecutive baseline pO_2 measurements were made over 24 min, while the rat breathed FO_2 = 33%. The inhaled gas was then sequentially altered to provide different inhaled FO_2, although the MF concentration was maintained constant at 0.5%. Inhaled gas was switched to 100% O_2 and pO_2 maps were immediately acquired with no equilibration period. Five consecutive maps were acquired over 40 min. The gas was then returned to baseline, followed by carbogen (95% O_2/5% CO_2), and finally, baseline again. In each case, gas was maintained for 40 min with five pO_2 determinations. The statistical significance of changes in oxygenation was assessed using an analysis of variance (ANOVA) on the basis of the Fisher's protected least significant difference (PLSD) test (Statview, SAS Institute, Cary, NC). Where appropriate, the Student's *t* test was applied.

Electrode measurements. After MRI measurement, one representative rat from each tumor subline was selected for electrode measurement using a non-Clark style oxygen needle electrode with a 0.7-mm-diameter tip (Product No. 768-22, Diamond General, Ann Arbor, MI) linked to a Chemical Microsensor (Diamond General). Calibration was performed using saline solutions equilibrated with air, 5% O_2, and 100% nitrogen at 37°C. After calibration, the needle electrode was inserted into the tumor, while a reference electrode was placed rectally. The pO_2 values were obtained at varying depths in two parallel tracks. In total, five locations in each tumor were studied. At each location within the tumor, the respiratory challenge sequence used for MRI was performed. After a change in inhaled gas, there was an equilibration period of 15 min and then pO_2 was recorded.

Immunohistochemistry

After MRI investigations, tumor tissues were surgically removed, fixed in 10% formalin for 24 h, and embedded in paraffin. Tissue sections (4 μm) were treated in boiling citrate buffer (0.1 M; pH 6.0) for 15 min and blocked in normal goat serum for 20 min. A primary antibody (1:50 dilution) against proliferating cell nuclear antigen (PCNA; BD Biosciences, San Diego, CA) was added and incubated overnight at 4°C in a humid box. Slides were then incubated with horseradish peroxidase (HRP)-conjugated goat anti-mouse secondary antibody (1: 100 dilution; Serotec, Raleigh, NC) for 1 h at 37°C. After a phosphate-buffered saline (PBS) wash, sections were immersed in the AEC substrate (3-amino-9-ethylcarbazole, Vector Laboratories, Inc., Burlingame, CA) for 15 min at room temperature. Finally, sections were counterstained with hematoxylin and mounted with Universal Mount. The positive and negative labeled nuclei were counted under microscopy. In total, 1000 nuclei were counted for each slide section; the labeling index was expressed as the percentage of positive cells for PCNA.

RESULTS

Histology shows distinctly different characteristics for the two sublines: the HI appears moderately well-differentiated with uniform sized tumor cells, pseudoglandular structures, and large vesicles (Fig. 1A). By comparison, the MAT-Lu appears poorly differentiated with cellular and nuclear variations in size and shape and no glandular structure (Fig. 1B). PCNA immunostaining also shows a higher proliferation rate in the MAT-Lu than the HI tumors (Fig. 1).

Hexafluorobenzene was readily observed by ^{19}F MRI after direct intratumoral injection, as shown for representative tumors in Fig. 2. Overlay of ^{19}F signal on the corre-

4|C

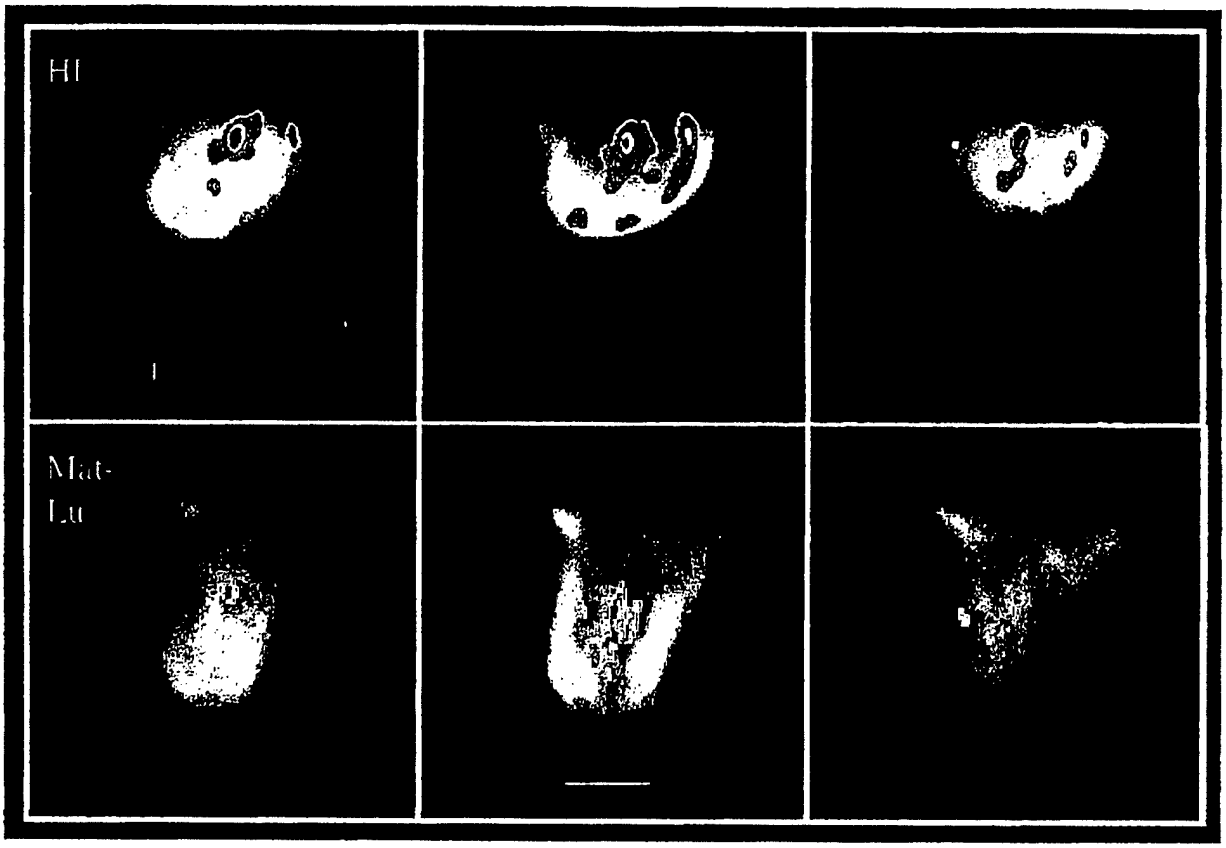

Fig. 2. MR images showing the distribution of hexafluorobenzene (45 μL) in representative large R3327 Dunning prostate rat tumors. Upper: HI (3.5 cm^3) and lower: MAT-Lu (3.8 cm^3). Three contiguous slices showing ^{19}F MRI signal density overlaid on the corresponding ^1H MR slices. HFB was detected from approximately 8% of the HI and 6% of the MAT-Lu tumor, predominantly in one plane. Each slice was 5 mm thick with in-plane resolution of 312 × 624 μm (^1H) or 312 × 1200 μm (^{19}F). Bar represents 1 cm.

sponding ^1H images indicates that HFB occurred in multiple discrete regions and was localized predominantly in the central slices with less signal in peripheral regions. In the series of EPI relaxation data sets, typically ~50–300 voxels provided an R1 fit, and potential pO_2 value. Because even noise may give an apparent relaxation curve (R1) fit, data were selected within a region of interest, and having T1 error < 2.5 s. With respect to respiratory interventions, only those voxels which provided consistently reliable data throughout all measurements were included for further analysis. The number of such acceptable voxels ranged from 18 to 84 per tumor.

F3 Figure 3 shows typical pO_2 maps of the selected regions obtained from the two tumors in Fig. 2. For the series of 23 pO_2 maps obtained with various inhaled gases, 39 voxels in the HI tumor and 52 voxels in the MAT-Lu tumor were considered reliable. Oxygen tension changed significantly when the rats inhaled oxygen or carbogen. Dynamic changes in mean pO_2 accompanying respiratory challenge
F4 in these two tumors are shown in Fig. 4. For the HI tumor, mean baseline pO_2 = 20 ± 5 (± SE) mm Hg (median pO_2 = 11 mm Hg), increased significantly within 8 min of switching the inspired oxygen from FO_2 = 33% to 100%, and the pO_2 reached 119 ± 10 mm Hg ($p < 0.0001$; median pO_2 = 58 mm Hg) after 40 min. Return to 33% O_2 produced a significant decline in pO_2 from the peak within 8 min, reaching a value of pO_2 = 33 ± 3 mm Hg by 40 min (median pO_2 = 39 mm Hg). Challenge with carbogen likewise produced a significant increase in pO_2 within 8 min and by 40 min reached a value of 113 ± 13 mm Hg ($p <$ 0.0001; median pO_2 = 60 mm Hg). Again pO_2 declined significantly upon returning to FO_2 = 33%. Baseline pO_2 in the MAT-Lu tumor was lower (mean = 11 ± 1 mm Hg; median = 8 mm Hg). But as with the HI, pO_2 steadily increased over 40 min upon altering inhaled gas to oxygen or carbogen (mean = 30 ± 3 mm Hg, median = 18 mm Hg; 47 ± 4 mm Hg, median pO_2 = 23 mm Hg, respectively; $p < 0.0001$). However, the mean values were always significantly lower than those in the size-matched HI tumor ($p < 0.0001$).

Data for small and large tumors in the HI and MAT-Lu sublines are pooled as histograms in Fig. 5 and summarized F5
in Table 1. Using the pooled data the small HI tumors had T1
a mean baseline pO_2 of 32 ± 1 mm Hg (median = 29 mm Hg), which was significantly greater than the larger HI tumors, which had a value of 14 ± 1 mm Hg (median = 7

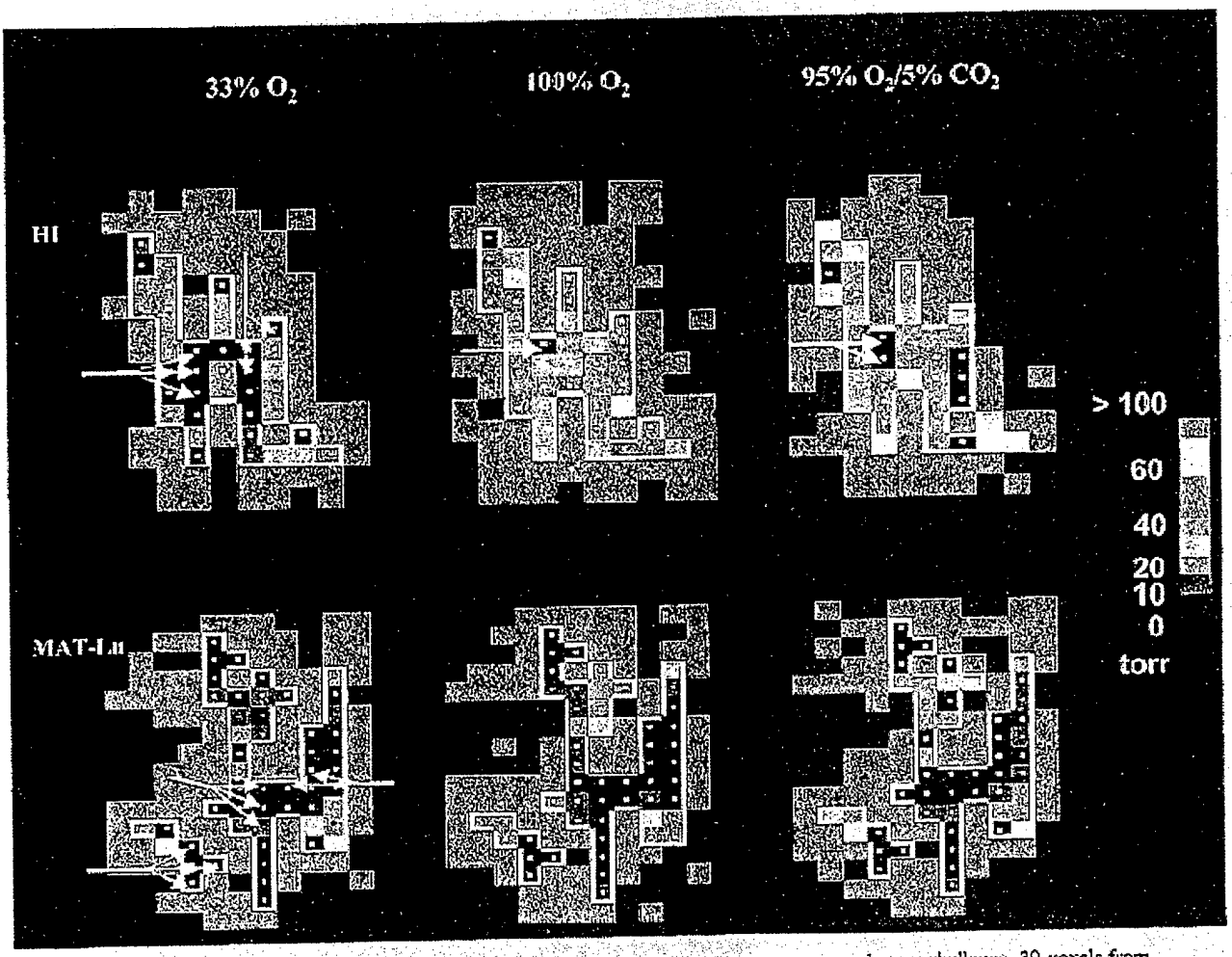

Fig. 3. pO_2 maps of selected regions from the tumors shown in Fig. 2 with respect to respiratory challenge. 39 voxels from the HI and 52 voxels from the MAT-Lu tumor were selected on the basis of consistently reliable data throughout all measurements. Maximum mean pO_2 increases with respect to respiratory challenges were found 40 min after breathing 100% oxygen or carbogen in both of these two tumors. Arrows indicate hypoxic voxels with $pO_2 < 10$ mm Hg.

mm Hg; $p < 0.0001$). For the MAT-Lu subline, small tumors had a mean pO_2 of 25 ± 1 mm Hg (median = 23 mm Hg), which was significantly greater than for the large MAT-Lu tumors (mean = 8 ± 1 mm Hg, median = 4 mm Hg; $p < 0.0001$). Comparison of the pooled mean baseline pO_2 between the two sublines showed that both the small and large groups of MAT-Lu tumors had significantly lower mean pO_2 than the size-matched HI groups ($p < 0.0001$; Table 1). All the tumors in the two sublines except one large MAT-Lu showed significant increases in global mean pO_2 with oxygen or carbogen inhalation ($p < 0.001$). In six of the seven HI tumors and five of the eight MAT-Lu tumors, the maximum mean pO_2 values were observed while the rats breathed carbogen. Most interestingly, hypoxic fraction, specifically $pO_2 < 10$ mm Hg (HF_{10}), in the large HI tumors decreased from 59% to 24% with oxygen and to 22% with carbogen inhalation, whereas in the large MAT-Lu tumors the final HF_{10} values were still over 37%. We also analyzed our pO_2 data by comparing the differences in individual tumors as shown in Table 2. As with the pooled data, for both the HI and MAT-Lu tumors, the large tumors were significantly more hypoxic when breathing 33% O_2 than the smaller tumors (Table 2). When breathing oxygen or carbogen, the mean and median pO_2 increased significantly for both the small and large HI tumors. The HF_{10} was significantly reduced in the large HI tumors. For the MAT-Lu tumors, the only significant change was an increase in the mean and median pO_2 in the large tumors with carbogen inhalation.

A major strength of the *FREDOM* approach is the ability to follow individual tumor regions. Thus, we selected those voxels from the baseline pO_2 maps, which were radiobiologically hypoxic ($pO_2 < 10$ mm Hg) in all three baseline measurements (24 min), to assess the influence of respiratory challenge. Inspection of the representative tumors in Fig. 3 shows that pO_2 increased significantly in the majority of the initially hypoxic voxels in the HI tumor ($p < 0.01$), whereas there was no significant response to oxygen or carbogen in the MAT-Lu. Data are summarized in Fig. 6.

For comparison, the traditional polarographic method

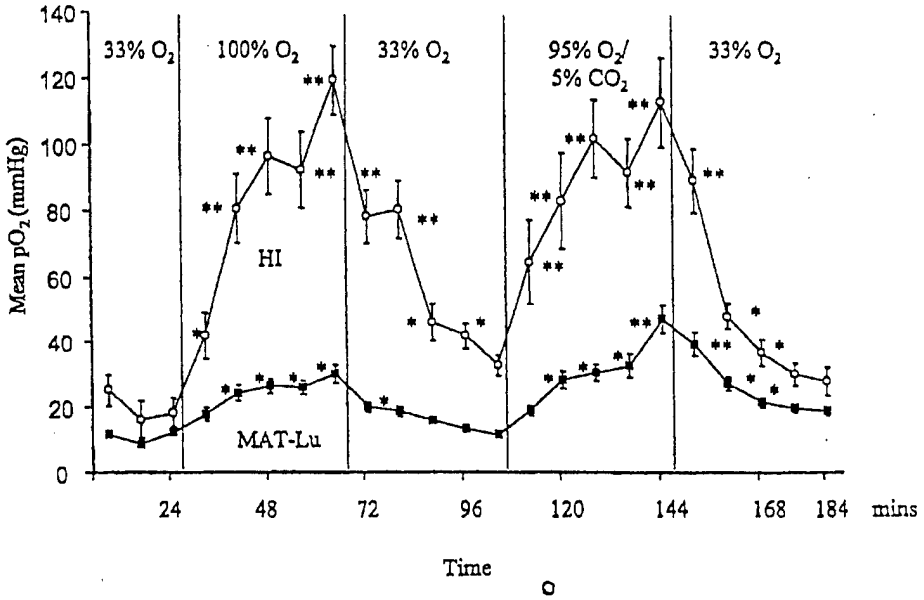

Fig. 4. Mean ± SE pO_2 obtained from sequential maps of the HI (□) and the MAT-Lu (■) tumors shown in Figs. 1 and 2 with respect to respiratory challenge. $*p < 0.001$, $**p < 0.0001$ compared to mean baseline.

was performed on one tumor from each subline after the NMR experiment (Fig. 7). All interrogated regions in the HI tumor, irrespective of baseline pO_2, showed a remarkable increase in pO_2 in response to oxygen or carbogen. However, only the relatively well-oxygenated regions (>10 mm Hg) in the MAT-Lu responded.

DISCUSSION

The oxygen tension dynamics observed here demonstrate that response to gaseous intervention can be very different for sublines of a single parental tumor type. The relatively hypoxic regions of the well-differentiated HI subline responded to elevated inhaled oxygen, whereas those of the undifferentiated MAT-Lu subline did not. Tumors of a given subline behaved consistently.

In common with our previous investigations of the undifferentiated anaplastic Dunning prostate R3327-AT1 subline (VDT ~5 days) (10, 11), we found that the larger tumors of each subline were significantly more hypoxic than smaller ones (Tables 1 and 2). Indeed, this is a general observation across most experimental tumor types, based on observations using various oximetry techniques (17–21), although exceptions have been reported (22). In response to respiratory challenge with oxygen or carbogen, as we also reported for the AT1 subline (11), for both the HI and MAT-Lu sublines the pooled data showed a significant increase in mean pO_2, irrespective of tumor size.

Under baseline conditions, the MAT-Lu tumors were significantly less well-oxygenated than the HI (Table 1). Large and small tumors responded to oxygen and carbogen, but MAT-Lu tumors consistently remained significantly less well-oxygenated than HI tumors. Further, the baseline radiobiologically hypoxic MAT-Lu voxels (<10 mm Hg) showed no significant increase in mean pO_2 (Fig. 6), a finding that coincides with our previous observations in the AT1 tumor (11, 23). In contrast, initially hypoxic voxels in the HI showed a rapid, and highly significant, response to respiratory challenge. This observation was confirmed using the traditional oxygen electrodes (Fig. 7), and previously using the fiber optic OxyLite (24). Such remarkable differences in behavior surely reflect intrinsic differences in the vascular architecture and perhaps the metabolic rate.

Previously, Eble *et al.* (13) compared oxygenation of the HI and undifferentiated AT1 (VDT ~5 days) Dunning prostate sublines using the Eppendorf Histograph. As we report here, they found that the slower growing, better differentiated tumor was better oxygenated. Likewise, Chapman *et al.* (22, 25, 26) found that the well-differentiated H subline (VDT 20 days) was better oxygenated than the AT1, as assessed by the Eppendorf electrode or by indirect means such as misonidazole binding and ^{31}P NMR. By contrast, Thews *et al.* (27) reported that a better differentiated rhabdomyosarcoma subline (F1) of the BA-HAN-1 was slightly less well-oxygenated than an undifferentiated counterpart subline (G8). While Thews' results show the opposite trend with differentiation, it is important to note that the F1 and G8 sublines each grow relatively rapidly (VDT 2.5–3 days). In the series of Dunning prostate tumors, VDTs range from 2.7 days (MAT-Lu) to 5 days (AT1), 9 days (HI), and 20 days (H). Comparing our current results with our own previous data from the undifferentiated AT1 with the same anesthesia protocol (10) reveals that correlations of hypoxia and growth rate or level of histologic differentiation are not always straightforward. Previously, we reported that smaller vs. larger AT1 tumors respectively

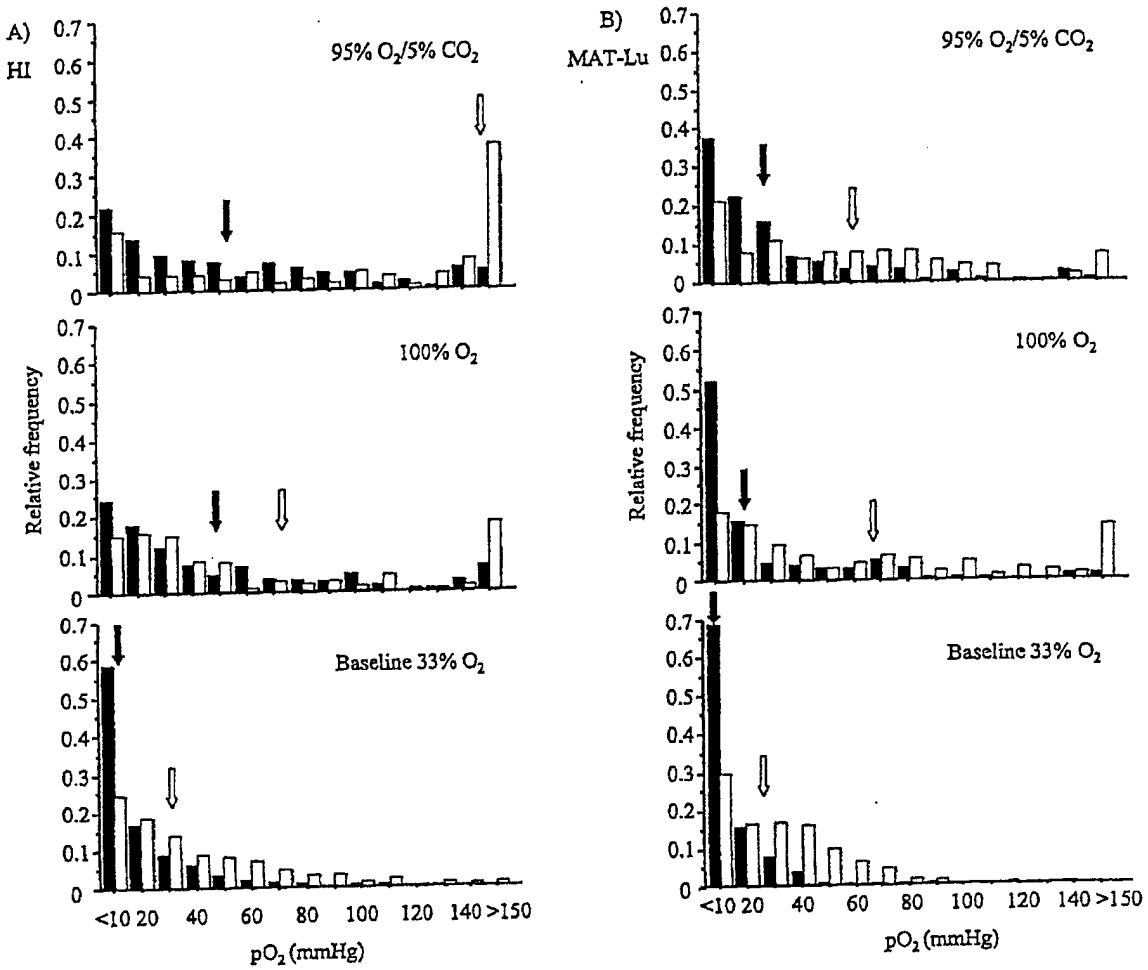

Fig. 5. Histograms of pooled pO_2 observed by *FREDOM* for all 15 tumors with respect to respiratory challenge. (A) Seven HI tumors including 4 large (solid) and 3 small (open). (B) Eight MAT-Lu tumors including 4 large (solid) and 4 small (open). Lowest frame: Rats inhaled 33% O_2. Middle frame: Maximum value when rats inhaled 100% O_2. Top frame: Maximum values when rats inhaled 95% O_2/5% CO_2. Arrows indicate mean values in large (solid) and small tumors (open), respectively.

had mean pO_2 = 39 vs. 3 torr, median pO_2 = 15 vs. 2 torr, and HF_{10} 44% and 82%. Thus, the AT1 apparently is more hypoxic than the MAT-Lu even though it grows more slowly. We believe the most valuable observation is that for both AT1 and MAT-Lu tumors, the initially hypoxic regions respond little to elevated oxygen inhalation, whereas the slower growing well-differentiated HI responds with a significant decline in HF_{10}. Thus, while growth rate and degree of differentiation each appear related to tumor oxygenation, we find the most pronounced effect is on the oxygen dynamics with respect to intervention.

In line with the observed VDT, histology using the proliferation marker PCNA showed a higher proliferation rate in the poorly oxygenated MAT-Lu than the relatively better oxygenated HI tumors. This result is in line with an *in vitro* study by Young *et al.* (28), who reported that hypoxia induced DNA overreplication. Likewise, Nordsmark *et al.* (29) reported that rapidly proliferating human soft tissue sarcomas from a clinical study were more hypoxic. Recent studies suggest that tumor hypoxia can enhance malignant progression and increase aggressiveness and metastasis (30, 31). In terms of the Dunning prostate R3327 rat tumors, Peschke *et al.* (14) found higher bromodeoxyuridine labeling in the fast growing and anaplastic AT1 subline compared with the slower growing and relatively well-differentiated H and HI sublines, which are relatively better oxygenated. However, some investigators have reported a lack of correlation between tumor oxygenation and proliferation in animals or patients (32). Future study regarding the relationship between these two factors is clearly needed. AQ: 3

Several reports based on the Eppendorf Histograph system have now shown that the level of hypoxia is related to clinical prognosis. Höckel *et al.* (33) found better disease-free and overall survival for patients with cervical cancer when median $pO_2 > 10$ mm Hg. Other reports have indicated similar findings, although alternate threshold parameters such as HF_5 (hypoxic fraction < 5 mm Hg) or $HF_{2.5}$ (hypoxic fraction < 2.5 mm Hg) have been favored over

Table 1. Summary of the pooled pO_2 data in R3327 Dunning prostate rat tumor sublines*

		Baseline (33% O_2)				Oxygen challenge				Carbogen challenge			
		pO_2 (mm Hg)		HF (%)		pO_2 (mm Hg)		HF (%)		pO_2 (mm Hg)		HF (%)	
				< 10	< 5			< 10	< 5			< 10	< 5
Tumor sublines	Size†	Mean ± SE	Median	mm Hg		Mean ± SE	Median	mm Hg		Mean ± SE	Median	mm Hg	
HI	Small	32 ± 1	29	24	16	75 ± 9‖	39	15	7	148 ± 12‖¶	111	16	5
	Large	14 ± 1‡	7	59	42	49 ± 4‡‖	26	24	13	53 ± 4‡‖	38	22	8
MAT-Lu	Small	25 ± 1§	23	30	21	68 ± 5§	44	18	12	63 ± 5§§	46	21	15
	Large	8 ± 1‡§	4	68	53	22 ± 4‡§‖	9	52	43	28 ± 4‡§‖	18	38	33

Abbreviation: HF = hypoxic fraction.

*The average number of voxels used to determine the mean and median pO_2 values for each gas was 198 for the small HI tumors, 226 for the large HI tumors, 229 for the small MAT-Lu tumors, and 148 for the large MAT-Lu tumors. These measurements reflect tumor size and tissue types irrespective of individual tumor, and indicate intratumoral heterogeneity.

†Small: volume < 2 cm^3; Large: volume > 3.5 cm^3.

‡$p < 0.0001$ from small.

§$p < 0.0001$ from HI.

‖$p < 0.0001$ from baseline.

¶$p < 0.0001$ from oxygen.

median value as a prognostic threshold (34, 35). Based on such findings, prospective clinical trials may now use pO_2 measurements for individual therapy planning. Clearly, the ability to differentiate those patients with well vs. poorly oxygenated tumors would be important in itself, but an even more powerful capability would be to assess the heterogeneity of the tumors and to determine whether hypoxic regions (voxels) are capable of responding to oxygen or carbogen.

There is increasing evidence suggesting that tumor metastasis may be associated with a hypoxic microenvironment (30, 31). An *in vivo* experimental study by Jaeger *et al.* showed that hypoxic murine KHT-C tumors are more likely to metastasize (36). Many clinical studies have also demonstrated a positive relationship between the presence of hypoxia and poor outcome associated with malignant progression and metastasis in several cancers, e.g., advanced squamous cell carcinoma of the cervix (33, 37), sarcomas and carcinomas from head, neck, and soft tissue (38). A hypoxic microenvironment is reported to induce increased expression of a group of genes, e.g., VEGF (vascular endothelial growth factor), PAI-1 (plasminogen activator inhibitor-1), and p53, which are associated with an increased malignant phenotype (39–42).

The clinical progression of prostatic cancer among patients remains by and large unpredictable. In some patients, the cancer metastasizes rapidly, killing the patient in less than a year, whereas in other patients the disease may remain localized for many years (43). Knowledge of the etiologic factors and biologic properties that predispose cells to malignant transformation remains essentially unknown (44). Thus, research that reveals factors, either temporal or causal, which can be linked to the onset of a metastatic potential, would surely be of great value. For instance, Movsas' study (45) using the Eppendorf Histograph reported that increasing levels of hypoxia were re-

Table 2. Comparison of pO_2 data in individual R3327 Dunning prostate rat tumors*

			Baseline (33% O_2)				Oxygen challenge				Carbogen challenge			
			pO_2 (mm Hg)		HF (%)		pO_2 (mm Hg)		HF (%)		pO_2 (mm Hg)		HF (%)	
					< 10	< 5			< 10	< 5			< 10	< 5
Tumor subline	Size†	No.	Mean ± SE	Median	mm Hg		Mean ± SE	Median	mm Hg		Mean ± SE	Median	mm Hg	
HI	Small	3	39 ± 11	38 ± 15	15 ± 3	11 ± 4	106 ± 40*§	68 ± 42	6 ± 3	5 ± 3	163 ± 64§	112 ± 10§	5 ± 3	3 ± 3
	Large	4	13 ± 3‡	7 ± 2‡	53 ± 4‡	40 ± 3‡	54 ± 14§	36 ± 11	20 ± 9§	14 ± 4§	58 ± 12§	41 ± 15	15 ± 8	10 ± 4
MAT-Lu	Small	4	24 ± 4	20 ± 5	23 ± 8	17 ± 7	60 ± 19	45 ± 20	14 ± 6	11 ± 6	59 ± 7	40 ± 14	14 ± 8	10 ± 5
	Large	4	8 ± 1‡	4 ± 1‡	58 ± 7‡	51 ± 8‡	27 ± 6	19 ± 7	40 ± 11	36 ± 10	43 ± 17§	39 ± 20§	34 ± 8	29 ± 6

Abbreviation: HF = hypoxic fraction.

*These data reflect individual tumors and provide an indication of intertumoral heterogeneity.

†Small: volume < 2 cm^3; Large: volume > 3.5 cm^3.

‡$p < 0.05$ from small.

§$p < 0.05$ from baseline.

rich3/2d-rob/2d-rob/2d-orig/2d9574d02a | destepha | S=3 | 4/11/02 | 12:19 | 4/Color Figure(s): 1,2,3 | Art: Biology contribution

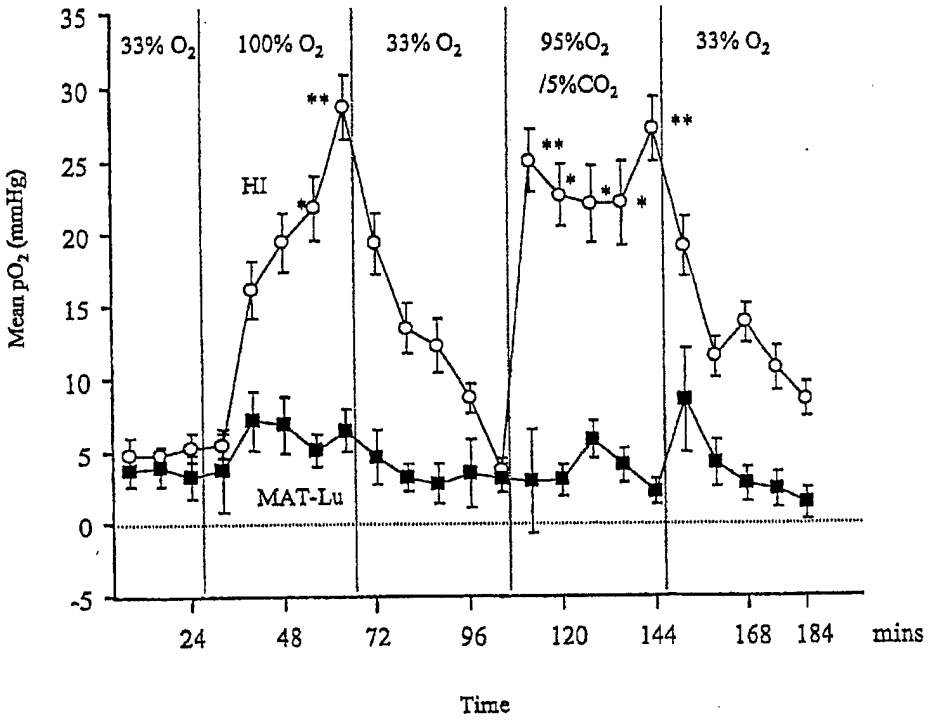

Fig. 6. Mean ± SE pO_2 in all the hypoxic voxels (<10 mm Hg) from each tumor in Fig. 2 with respect to respiratory challenge. (A) Significant increases in mean pO_2 of the 7 hypoxic HI (❑) voxels in response to 100% O_2 or 95% O_2/5% CO_2 challenge (*$p < 0.05$; **$p < 0.01$). (B) No increase was observed in mean pO_2 of the 10 hypoxic MAT-Lu (■) voxels.

lated to increasing clinical stage of human prostate carcinomas. This finding may simply support our findings, relating increasing size to greater tumor hypoxia. In the present study, we chose to compare the moderately well-differentiated HI and poorly differentiated and highly metastatic MAT-Lu sublines, both derived from Dunning R3327 prostatic tumor (15), to investigate the extent of hypoxia. This study was not designed to investigate the correlation between hypoxia and tumor malignant progression, but clearly there is a need for further investigation to separate the phenotypic characteristics of differentiation, growth rate, and metastatic tendency. We propose to undertake further studies comparing the Dunning prostate AT2.1, AT6.3, and G sublines (4) to test these issues.

Many experimental and clinical studies have demonstrated that reoxygenation of hypoxic tumor cells contributes to improved radiation sensitivity for tumor therapy (46, 47). Therefore, how this population of cells responds to respiratory challenge is particularly important. If the findings we present here are confirmed in prostate cancer patients, it would suggest therapeutic value of monitoring tumor baseline and dynamic pO_2. Tumors like the HI can be modulated and might be expected to show improved response to radiotherapy with oxygen or carbogen inhalation before therapy; in tumors like MAT-Lu one might expect little advantage, indicating a need for an alternative approach.

In recent clinical trials, carbogen has been favored over oxygen, as an adjuvant intervention to enhance radiotherapy. Here, except in the small HI tumors, which exhibited significantly higher mean pO_2 in response to carbogen than oxygen, we have found no significant difference between the two gases, in terms of pO_2 values and hypoxic fraction. A recent report by Hartmann *et al.* (48) showed that hyperbaric oxygen, but not carbogen, significantly increased the median pO_2, leading to better radiation response in the rhabdomyosarcoma R1H. Further studies will be required to validate this observation, including reversing the order of administered gases, since a conditioning effect could have been generated here. We also note that changes in pO_2 were still occurring at 40 min, when we ceased our interventions here (Fig. 4). Others have reported a differential response to oxygen or carbogen in clinical gynecological tumors, where inhalation of either gas elevated median and mean pO_2, but only carbogen was effective at eliminating the hypoxic fraction (49). Such an observation was also reported for human glioma xenografts (50). Others have reported that response can depend on tumor type and site of implantation (51). In some cases, vasoactive agents have been shown to have differential activity against small and large tumors; e.g., angiotensin II led to reduced pO_2 in small DS-sarcomas ($0.75\ cm^3$), but increased pO_2 in larger tumors ($1.8\ cm^3$) (21). This was attributed to the relative role of preexisting host vessels vs. newly formed vessels lacking innervation and a responsive musculature. Here, in the HI tumor, we see that carbogen was equally effective in small or large tumors,

AQ: 5

HI

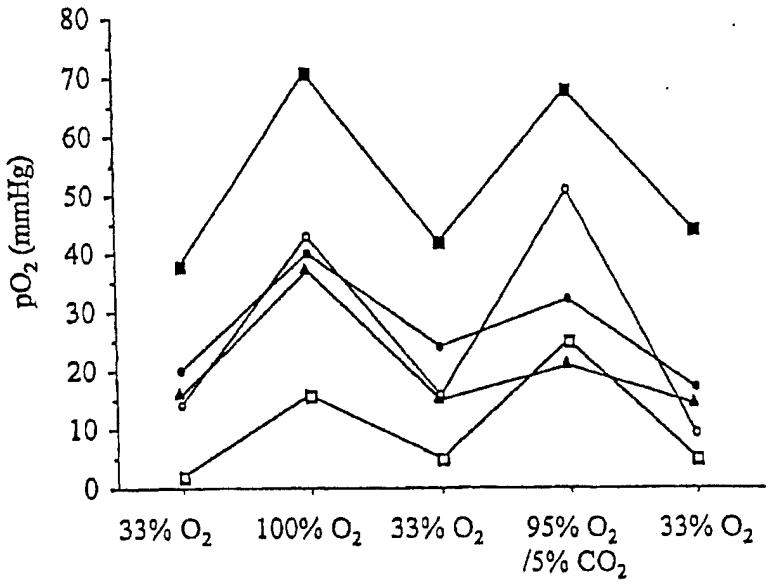

MAT-Lu

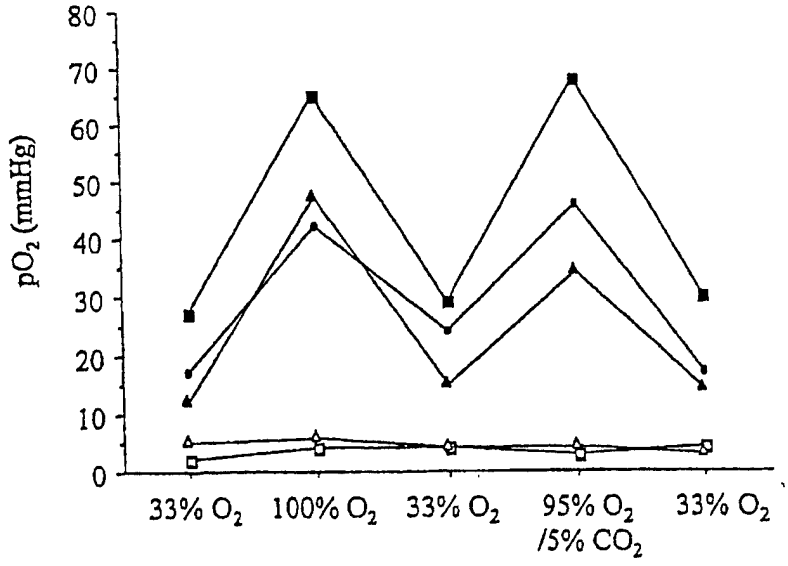

Fig. 7. Electrode measurements of pO_2 in one large tumor from each subline. pO_2 values in five locations in each tumor were measured with respiratory challenge. pO_2 in all the locations in the HI tumor increased remarkably with 100% O_2 or carbogen. In the MAT-Lu tumor, regions with initial $pO_2 > 10$ mm Hg responded significantly, whereas those relatively hypoxic did not.

consistent with the highly differentiated morphology and well-developed vasculature. Data obtained for the HI tumor here are very similar to results obtained previously with this tumor subline when rats were breathing an alternative anesthetic (isoflurane in air) (24). The extensive heterogeneity within tumors emphasizes the importance of an imaging approach to examining differential oxygen dynamics. Here, we have used an oxygen electrode to validate the magnitude of changes observed in tumors, and previously we have shown that observation based on optical fiber probes (OxyLite) also gave consistent data (24).

Comparison of repeat measurements with respect to acute

interventions is predicated on reproducibility. We have previously shown that individual baseline pO_2 measurements are usually stable for at least 1 h (10, 52). It has also been shown that pO_2 distributions in tumors are stable over several hours even with respect to repeat anesthesia episodes and movement of the rats out and back into an MRI system (53). We have, however, noted that HFB clears from tumors with a typical half-life of 600 min, and thus, we apply the *ARDVARC* data acquisition protocol to minimize any systematic errors in pO_2 measurements during the 8-min acquisition period. We have shown that there is little macroscopic redistribution over a period of 2.5 h (12).

In agreement with most reports on tumors implanted in rats or mice, we have found that large tumors are significantly more hypoxic. Some clinical studies have failed to show such a correlation. Our recent results (24) from a series of HI tumors, which we followed chronologically for a period of weeks with respect to increasing size, showed a catastrophic fall in pO_2 at some stage between 1 and 2 cm^3. Beyond this size, tumors remained poorly oxygenated. We note that most clinical tumors are much larger, usually >5 cm^3 and sometimes reaching 50 to 100 cm^3 and they may therefore already be at a low pO_2 plateau. We note that some clinical studies have shown a correlation between size and oxygenation (34, 54, 55) and Movsas *et al.* (45) using the Eppendorf Histograph reported a correlation between hypoxia and tumor stage in the prostate.

Limited ketamine (200 μL) was given to each rat i.p. as a relaxant before MR studies. It has been reported that ketamine does not affect mean arterial pressure, heart rate, or cerebral artery blood flow (56). However, methoxyflurane may cause a depression of respiration, tumor blood flow, and heart rate (57). Anesthesia is required to minimize stress and ensure no movement during imaging procedures. Immobilized tumors are vital to allow sequential correlation of specific tumor regions during investigations. Because all rats received the same constant level of anesthesia, we believe that it does not compromise or bias our observations and comparison of different tumor types. Recently, we have switched to isoflurane (24), which may be less vasoactive (57), but we find that HI tumors behave similarly with respect to either anesthesia.

Although we have thus far limited our application of the *FREDOM* approach to fundamental questions of tumor biology in animals, we believe the technique is ready for translation to the clinic. HFB is readily available, exhibits remarkably low toxicity, and could be easily administered to tumors on or near the surface of the body. *FREDOM* is analogous to use of the Eppendorf Histograph in terms of inserting a needle into a tumor, although our needle is considerably finer and no further needle insertion is required for repeated measurements when taken over the next few hours. In terms of patient compliance, Aquino-Parsons *et al.* (49) have already used the Eppendorf Histograph for up to three repeat measurements with respect to respiratory interventions in women with cervical cancer. *FREDOM* does involve sampling a limited region of the tumor by injection of the HFB reporter. However, we have previously shown that pO_2 distributions are similar to those achieved with the Eppendorf Histograph (10). Appropriate injection protocols are required to avoid bias, although for dynamic studies, as presented here, this is less important because each voxel serves as its own control.

To avoid violating the tumor itself, we have previously tested i.v. administration of perfluorocarbon emulsions as reporter molecules (58). However, we and others (58–60) showed that measurements are biased toward well-perfused tumor regions. Histology can be applied to intrinsic markers of hypoxia (61, 62), but this requires biopsy. Moreover, sampling is still involved both in terms of selecting the biopsy site and then choosing representative tissue slices and microscopic fields. Thus, we believe that *FREDOM* is competitive with many current or proposed invasive clinical techniques. While we believe that *FREDOM* is very valuable for animal research and has great potential in the clinic, we are nonetheless also investigating alternative approaches to measuring tumor oxygenation (63, 64). The BOLD approach (9) is very appealing, providing rapid noninvasive images, but quantitative measurements of signal dynamics provide only a qualitative indication of tumor oxygenation; much research remains to be done to relate the observed signal changes to therapeutic outcome. Near-infrared approaches can also interrogate tumor vasculature noninvasively, but hitherto, they have been limited to global observations, providing an indication of average tumor vascular oxygenation only (63).

In conclusion, we have demonstrated that, in comparison with the HI tumor, the faster growing and poorly differentiated MAT-Lu subline of the Dunning R3327 tumor is significantly more hypoxic and the level of hypoxia increases in both sublines with increasing size. Most significantly, we have demonstrated that two tumors derived from the same original parental tumor respond differently to an intervention. This emphasizes the need to assess individual tumors in the clinic in order to optimize a therapeutic regime.

REFERENCES

1. Brown JM. The hypoxic cell: A target for selective cancer therapy—eighteenth Bruce F. Cain memorial award lecture. *Cancer Res* 1999;59:5863–5870.
2. Hall EJ. The oxygen effect and reoxygenation. In: Hall EJ, editor. Radiobiology for the radiologist. Philadelphia: Lippincott; 1994. p. 133–152.
3. Chapman JD, Stobbe CC, Arnfield MR, *et al.* Oxygen dependency of tumor cell killing *in vitro* by light activated photofrin II. *Radiat Res* 1991;126:73–79.
4. Zhong H, Agani F, Baccala AA, *et al.* Increased expression of hypoxia inducible factor-1 alpha in rat and human prostate cancer. *Cancer Res* 1998;58:5280–5284.
5. Rofstad EK, Danielsen T. Hypoxia-induced metastasis of human melanoma cells: Involvement of vascular endothelial

growth factor-mediated angiogenesis. *Br J Cancer* 1999;80: 1697–1707.

6. Stone HB, Brown JM, Phillips T, *et al.* Oxygen in human tumors: Correlations between methods of measurement and response to therapy. *Radiat Res* 1993;136:422–434.
7. Sostman HD, Rockwell S, Sylva AL, *et al.* Evaluation of BA 1112 rhabdomyosarcoma oxygenation with microelectrodes, optical spectrometry, radiosensitivity, and MRS. *Magn Reson Med* 1991;20:253–267.
8. Vaupel P, Kelleher DK, Engel T. Stable bioenergetic status despite substantial changes in blood flow and tissue oxygenation in a rat tumour. *Br J Cancer* 1994;69:46–49.
9. Robinson SP, Collingridge DR, Howe FA, *et al.* Tumor response to hypercapnia and hyperoxia monitored by FLOOD magnetic resonance imaging. *NMR Biomed* 1999;12:98–106.
10. Mason RP, Constantinescu A, Hunjan S, *et al.* Regional tumor oxygenation and measurement of dynamic changes. *Radiat Res* 1999;152:239–249.
11. Hunjan S, Zhao D, Constantinescu A, *et al.* Tumor oximetry: Demonstration of an enhanced dynamic mapping procedure using fluorine-19 echo planar magnetic resonance imaging in the Dunning prostate R3327-AT1 rat tumor. *Int J Radiat Oncol Biol Phys* 2001;49:1097–1108.
12. Mason RP, Rodbumrung W, Antich PP. Hexafluorobenzene: A sensitive ^{19}F NMR indicator of tumor oxygenation. *NMR Biomed* 1996;9:125–134.
13. Eble MJ, Lohr F, Wenz F, *et al.* Tissue oxygen tension distribution in two sublines of the Dunning prostate tumor R3327. In: Vaupel PW, Kelleher DK, Gunderoth M, editors. Tumor oxygenation. Gustav Fischer Verlag, Stuttgart: Funktionsanalyse Biologischer Systeme; 1995. p. 95–105.
14. Peschke P, Hahn EW, Wenz F, *et al.* Differential sensitivity of three sublines of the rat Dunning prostate tumor system R3327 to radiation and/or local tumor hyperthermia. *Radiat Res* 1998;150:423–430.
15. Isaacs J, Isaacs W, Feitz W, *et al.* Establishment and characterization of 7 Dunning prostate cancer cell lines and their use in developing methods for predicting metastatic ability of prostate cancer. *Prostate* 1986;9:261–281.
16. Hahn EW, Peschke P, Mason RP, *et al.* Isolated tumor growth in a surgically formed skin pedicle in the rat: A new tumor model for NMR studies. *Magn Reson Imaging* 1993;11:1007–1017.
17. Vaupel PW, Fortmeyer HP, Runkel S, *et al.* Blood flow, oxygen consumption, and tissue oxygenation of human breast cancer xenografts in nude rats. *Cancer Res* 1987;47:3496–3503.
18. Terris DJ, Minchinton AI, Dunphy EP, *et al.* Computerized histographic oxygen tension measurement of murine tumors. In: Erdmann E, Bruley DF, editors. Oxygen transport to tissue XIV. New York: Plenum; 1992. p. 153–159.
19. Baldwin NJ, Ng TC. Oxygenation and metabolic status of KHT tumors as measured simultaneously by ^{19}F magnetic resonance imaging and ^{31}P magnetic resonance spectroscopy. *Magn Reson Imaging* 1996;14:514–551.
20. Shibamoto Y, Yukawa Y, Tsutsui K, *et al.* Variation in the hypoxic fraction among mouse tumors of different types, size, and site. *Jpn J Cancer Res* 1986;77:908–915.
21. Thews O, Kelleher DK, Vaupel P. Disparate responses of tumour vessels to angiotensin II: Tumour volume-dependent effects on perfusion and oxygenation. *Br J Cancer* 2000;83: 225–231.
22. Yeh KA, Biade S, Lanciano RM, *et al.* Polarographic needle electrode measurements of oxygen in rat prostate carcinomas: Accuracy and reproducibility. *Int J Radiat Oncol Biol Phys* 1995;33:111–118.
23. Hunjan S, Mason RP, Constantinescu A, *et al.* Regional tumor oximetry: ^{19}F NMR spectroscopy of hexafluorobenzene. *Int J Radiat Oncol Biol Phys* 1998;40:161–171.
24. Zhao D, Constantinescu A, Hahn EW, *et al.* Tumor oxygen dynamics with respect to growth and respiratory challenge: Investigation of the Dunning prostate R3327-HI tumor. *Radiat Res* 2001;156:510–520.
25. Thorndyke C, Meeker B, Thomas G, *et al.* The radiation sensitivities of R3327-H and -AT1 rat prostate adenocarcinomas. *J Urol* 1985;134:191–198.
26. Chapman JD, Engelhardt EL, Stobbe CC, *et al.* Measuring hypoxia and predicting tumor radioresistance with nuclear medicine assays. *Radiother Oncol* 1998;46:229–237.
27. Thews O, Kelleher DK, Lecher B, *et al.* Blood flow, oxygenation, metabolic and energetic status in different clonal subpopulations of a rat rhabdomyosarcoma. *Int J Oncol* 1998;13: 205–211.
28. Young S, Marshall R, Hill R. Hypoxia induces DNA overreplication and enhances metastatic potential of murine tumor cells. *Proc Natl Acad Sci USA* 1988;85:9533–9537.
29. Nordsmark M, Hoyer M, Keller J, *et al.* The relationship between tumor oxygenation and cell proliferation in human soft tissue sarcomas. *Int J Radiat Oncol Biol Phys* 1996;35: 701–708.
30. Höckel M, Vaupel P. Tumor hypoxia: Definitions and current clinical, biologic, and molecular aspects. *J Natl Cancer Inst* 2001;93:266–276.
31. Rofstad EK. Microenvironment-induced cancer metastasis. *Int J Radiat* 2000;76:589–605.
32. Raleigh JA, Zeman EM, Calkins DP, *et al.* Distribution of hypoxia and proliferation associated markers in spontaneous canine tumors. *Acta Oncol* 1995;34:849–853.
33. Höckel M, Schlenger K, Aral B, *et al.* Association between tumor hypoxia and malignant progression in advanced cancer of the uterine cervix. *Cancer Res* 1996;56:4509–4515.
34. Fyles AW, Milosevic M, Wong R, *et al.* Oxygenation predicts radiation response and survival in patients with cervix cancer. *Radiother Oncol* 1998;48:149–156.
35. Nordsmark M, Overgaard M, Overgaard J. Pretreatment oxygenation predicts radiation response in advanced squamous cell carcinoma of head and neck. *Radiother Oncol* 1996;41: 31–39.
36. Jaeger KD, Kavanagh M-C, Hill RP. Relationship of hypoxia to metastatic ability in rodent tumors. *Br J Cancer* 2001;84: 1280–1285.
37. Birner P, Schindl P, Obermair A, *et al.* Overexpression of hypoxia-inducible factor 1 is a marker for an unfavorable prognosis in early-stage invasive cervical cancer. *Cancer Res* 2000;60:4693–4696.
38. Brizel DM, Scully SP, Harrelson JM, *et al.* Tumor oxygenation predicts for the likelihood of distant metastases in human soft tissue sarcoma. *Cancer Res* 1996;56:941–943.
39. Giaccia AJ. Hypoxic stress proteins: Survival of the fittest. *Semin Radiat Oncol* 1996;6:46–58.
40. Heacock CS, Sutherland RM. Induction characteristics of oxygen regulated proteins. *Int J Radiat Oncol Biol Phys* 1986; 12:1287–1290.
41. Graeber TG, Osmanian C, Jacks T, *et al.* Hypoxia-mediated selection of cells with diminished apoptotic potential in solid tumours. *Nature* 1996;379:88–91.
42. Koong AC, Denko NC, Hudson KM, *et al.* Candidate genes for the hypoxic tumor phenotype. *Cancer Res* 2000;60:883–887.
43. Catalona WJ, Scott WW. Carcinoma of the prostate. In: Harrison JH, editor. Cancer urology. Philadelphia: WB Saunders; 1979. p. 1085–1124.
44. Chiarado A. National Cancer Institute roundtable on prostate cancer: Future research direction. *Cancer Res* 1991;51:2498–2505.

45. Movsas B, Chapman J, Horwitz E, *et al.* Hypoxic regions exist in human prostate carcinoma. *Urology* 1999;53:11–18.
46. Kallman R, Dorie M. Tumor oxygenation and reoxygenation during radiation therapy: Importance in predicting tumor response. *Int J Radiat Oncol Biol Phys* 1986;12:681–685.
47. Fenton BM. Effects of carbogen plus fractionated irradiation on KHT tumor oxygenation. *Radiother Oncol* 1997;44:183–190.
48. Hartmann K, van der Kleij A, Carl U, *et al.* Effects of hyperbaric oxygen and normobaric carbogen on the radiation response of the rat rhabdomyosarcoma R1H. *Int J Radiat Oncol Biol Phys* 2001;51:1037–1044.
49. Aquino-Parsons C, Green A, Minchinton AI. Oxygen tension in primary gynaecological tumours: The influence of carbon dioxide concentration. *Radiother Oncol* 2000;57:45–51.
50. van der Sanden BJP, Heerschap A, Hoofd L, *et al.* Effect of carbogen breathing on the physiological profile of human glioma xenografts. *Magn Reson Med* 1999;42:490–499.
51. Lanzen JL, Braun RD, Ong AL, *et al.* Variability in blood flow and pO_2 in tumors in response to carbogen breathing. *Int J Radiat Oncol Biol Phys* 1998;42:855–859.
52. Le D, Mason RP, Hunjan S, *et al.* Regional tumor oxygen dynamics: ^{19}F PBSR EPI of hexafluorobenzene. *Magn Reson Imaging* 1997;15:971–981.
53. Hunjan S. In-vivo fluorine nuclear magnetic resonance investigations of tumor oxygen tension and pH [Ph.D. dissertation]. Dallas: University of Texas Southwestern Medical Center; 1999.
54. Lartigau E, Le Ridant AM, Lambin P, *et al.* Oxygenation of head and neck tumors. *Cancer* 1993;71:2319–2325.
55. Hohenberger P, Felger C, Haensch W, *et al.* Tumor oxygenation correlates with molecular growth determinants in breast cancer. *Breast Cancer Res Treatment* 1998;48:97–106.
56. Sasaki K, Cho S, Fukusaki M, *et al.* The effects of propofol with and without ketamine on human cerebral blood flow velocity and CO_2 response. *Anesth Analg* 2000;90:377–382.
57. McKelvey D. Halothane, isoflurane, and methoxyflurane: Physical properties and pharmacology. *Veterinary Technician* 1991;12:21–28.
58. Mason RP, Antich PP, Babcock EE, *et al.* Non-invasive determination of tumor oxygen tension and local variation with growth. *Int J Radiat Oncol Biol Phys* 1994;29:95–103.
59. McIntyre DJO, McCoy CL, Griffiths JR. Tumor oxygenation measurements by ^{19}F MRI of perfluorocarbons. *Curr Sci* 1999;76:753–762.
60. van der Sanden BPJ, Heerschap A, Simonetti AW, *et al.* Characterization and validation of non-invasive oxygen tension measurements in human glioma xenografts by 19F-MR relaxometry. *Int J Radiat Oncol Biol Phys* 1999;44:649–658.
61. Semenza GL. Hypoxia, clonal selection, and the role of HIF-1 in tumor progression. *Crit Rev Biochem Mol Biol* 2000;35:71–103.
62. Loncaster JA, Harris AL, Davidson SE, *et al.* Carbonic anhydrase (CA IX) expression, a potential new intrinsic marker of hypoxia: Correlation with tumor oxygen measurement and prognosis in locally advanced carcinoma of the cervix. *Cancer Res* 2001;61:6394–6399.
63. Liu H, Song Y, Worden KL, *et al.* Noninvasive investigation of blood oxygenation dynamics of tumors by near-infrared spectroscopy. *Appl Optic* 2000;39:5231–5243.
64. Fink K, Yetkin Z, McColl R, *et al.* Brain tumor vascular dynamics: A BOLD MRI investigation. 92nd AACR, New Orleans, LA; 2001. p. 388. (Abstr). AQ: 8

Correlation of tumor oxygen dynamics with radiation response of the Dunning prostate R3327-HI tumors*

Dawen Zhao[1], Anca Constantinescu[1], Cheng-Hui Chang[2], Eric W. Hahn[1], and Ralph P. Mason[1 a]

[1]Advanced Radiological Sciences, Department of Radiology; and [2] Department of Radiation Oncology,

The University of Texas Southwestern Medical Center, Dallas, Texas

Number of copies: 5

Number of figures: 6

Running title header: Oxygen dynamics predict radiosensitivity

Keywords: oxygen tension, fluorine magnetic resonance imaging, radiosensitivity, prostate tumor, hypoxia.

* Presented in part at the 48th Annual Radiation Research Society Meeting, San Juan, Puerto Rico, April 2001.

[a] Address correspondence to:

Ralph P. Mason, Ph.D., C. Chem.,

Department of Radiology,

U.T. Southwestern Medical Center,

5323 Harry Hines Blvd.,

Dallas, TX 75390-9058

Tel: (214) 648-8926; Fax: (214) 648-2991;

E. mail: Ralph.Mason@UTSouthwestern.edu

Zhao, D., Constantinescu, A., Hahn, E. W. and Mason, R. P. Correlation of tumor oxygen dynamics with radiation response of the Dunning prostate R3327-HI tumors. *Radiat. Res.*

Abstract

Our previous studies have shown that oxygen inhalation significantly reduces tumor hypoxia in the moderately well differentiated HI subline of the Dunning prostate R3327 rat carcinoma. To test our hypothesis that modifying hypoxia could improve radiosensitivity of these tumors, we performed experimental radiotherapy to compare the tumor response to ionizing radiation alone or in combination with oxygen inhalation. Tumor pO_2 measurements were performed on size selected tumors several hours before radiotherapy using ^{19}F nuclear magnetic resonance echo planar imaging relaxometry (*FREDOM*) of the reporter molecule hexafluorobenzene. In common with our previous findings, the larger tumors (> 3.5 cm^3) exhibited greater hypoxia than the smaller tumors (< 2 cm^3; $p < 0.001$), and oxygen inhalation reduced the hypoxic fraction (< 10 torr): in the larger tumors, hypoxic fraction dropped significantly from a mean baseline value 77% to 17% ($p < 0.001$). The effect of oxygen, administered 30 min before and during irradiation, on tumor response to a single 30 Gy dose of photons was evaluated by growth delay. For the smaller tumors no difference in growth delay was found when treatment occurred with or without oxygen breathing. By contrast, breathing oxygen before and during irradiation produced a significantly enhanced growth delay in the larger tumors (enhancement ratio = 2.4). The differential behavior may be attributed to the low baseline hypoxic fraction (< 10 torr) in small tumors (20%) as a target for oxygen inhalation. Our histological studies showed a good match between the perfused vessels marked by Hoechst 33342 dye and the total vessels immunostained by anti-CD31 and indicated extensive perfusion in this tumor line. In summary, the present results suggest that the ability to detect modulation of tumor pO_2, in particular, the residual hypoxic fraction, with respect to an intervention, could have prognostic value for predicting the efficacy of radiotherapy.

Introduction

It is recognized that measurement of pretreatment tumor oxygenation can have prognostic value (*1-3*), and increased tumor pO_2 promotes radiosensitivity (*4, 5*). Many adjuvant interventions have been tested to manipulate tumor oxygenation in order to improve response to irradiation, *e.g.*, normobaric or hyperbaric oxygen breathing, carbogen alone or combined with nicotinamide, infusion of blood substitutes, and hemoglobin-oxygen affinity modifiers (*3, 6*). While the beneficial effects of such modifiers have sometimes been translated from animal to clinical studies (*7, 8*), many clinical trials have failed to show therapeutic benefit (*9*). This has often been attributed to the inability to identify those patients who would benefit from adjuvant intervention or sub-optimal timing of such intervention (*3*).

Accurate evaluation of pretreatment tumor oxygenation and its response to adjuvant intervention may allow therapy to be tailored to individual characteristics. To date the Eppendorf Histograph has been most widely used to measure tumor pO_2 in both experimental and clinical studies and disease free survival has been correlated with hypoxia in studies of cervical cancer (*1, 2*) and head and neck cancer (*10-12*). The Eppendorf has been considered by some as a 'gold standard' for pO_2 measurement, but it is impractical for longitudinal studies of specific regions of interest. Longitudinal imaging studies with respect to intervention are already performed in experimental superficial tumors, *e.g.* window chamber models, but investigations of deeper tissues have been relatively elusive. Historically, electrodes (*13*), or more recently fiber optic probes (*14*), or electron spin resonance (*15*) have been applied to examine dynamic changes at a few (1-4) limited locations. Blood Oxygen Level Dependent (BOLD) contrast proton MRI is a completely noninvasive technique to assess tumor vascular oxygenation and heterogeneity in response to intervention, but the method does not provide pO_2 values and interpretation may be complicated by flow (*16*).

We have established an MRI approach to measure tumor oxygen tension quantitatively at multiple locations simultaneously: *FREDOM* (Fluorocarbon Relaxometry using Echo planar imaging for Dynamic Oxygen Mapping) with hexafluorobenzene (HFB), as a reporter molecule (*17, 18*). This technique allows us both to assess baseline pO_2 at multiple specific locations simultaneously within a tumor and also to

follow dynamic changes in response to interventions. Our previous work (*19, 20*) using *FREDOM* showed differential size-related oxygenation of the relatively slow growing, moderately well differentiated Dunning prostate R3327 HI rat tumor. Most importantly, we found that oxygen inhalation significantly decreased tumor hypoxia in the HI tumor irrespective of baseline hypoxia. Thus the HI tumor appeared to be an ideal model to test whether our measurements of tumor oxygen dynamics could be correlated with therapeutic outcome.

Methods

Experiments were approved by the Institutional Animal Care and Research Advisory Committee.

Tumor Model

Syngeneic Dunning prostate R3327-HI tumors, a moderately well differentiated and relatively slow growing subline with tumor volume doubling time (VDT) of 9 days (*21, 22*) were originally obtained from Dr. J.T. Isaacs, Johns Hopkins University. Tumors were implanted in surgically formed skin pedicles on the foreback of adult male Copenhagen-2331 rats (Harlan, Indianapolis, IN; ~250 g), as described in detail previously (*23*). Thirty-six tumors were examined: grouped at time of initial measurement as sixteen smaller tumors (< 2 cm^3; mean = 1.4 ± 0.1 cm^3) and twenty larger tumors (> 3.5 cm^3; mean = 6.4 ± 0.7 cm^3).

Tumor Oximetry - FREDOM

Four small tumors and six larger tumors were used for MRI studies, which were performed as described in detail previously (*19*). Briefly, each rat was given 200 µl ketamine hydrochloride (100 mg/ml, Aveco, Fort Dodge, IA) as a relaxant (i.p.) and maintained under general gaseous anesthesia [air and 1.3% isoflurane (Baxter International Inc., Deerfield, IL)]. Hexafluorobenzene (45 µl; Lancaster, Gainesville, FL), which had been deoxygenated by bubbling nitrogen for 5 mins before use, was injected directly into the tumors using a Hamilton syringe (Reno, NV) with a custom-made fine sharp needle (32G). The HFB was deliberately deposited in both the central and peripheral regions of the tumors to ensure that the interrogated regions would be representative of the whole tumor. Generally, HFB was administered along

two or three tracks in the form of a fan in a single central plane of the tumor sagittal to the rat's body. Each animal was placed on its side in a cradle with a thermal blanket to maintain body temperature.

Magnetic resonance experiments were performed using an Omega CSI 4.7 horizontal bore magnet system with actively shielded gradients (Bruker Instrument Inc., Fremont, CA). A tunable ($^{1}H/^{19}F$) single-turn solenoid coil (2 or 3.5 cm in diameter to generally accommodate the tumor size) was placed around the tumor-bearing pedicle and ^{1}H (200.1 MHz) and ^{19}F (188.3 MHz) images were obtained using three-dimensional (3D) spin-echo sequences to reveal the distribution of HFB within the tumors. Following conventional MR imaging, tumor oxygenation was estimated using *FREDOM* on the basis of ^{19}F pulse burst saturation recovery (PBSR) echo planar imaging (EPI) relaxometry of the HFB (*18*). pO_2 maps with 1.25 mm in plane voxel resolution were obtained in 8 minutes. The spin-lattice relaxation rate [$R1(s^{-1})$ = 1/T1] was estimated on a voxel-by-voxel basis using a three-parameter monoexponential function, and pO_2 was estimated using the relationship pO_2 (torr) = (R1 – 0.0835)/0.001876 (*18*). Typically, ~100-300 voxels provided an R1 fit, and potential pO_2 value. Since noise itself may give an apparent relaxation curve (R1) fit, data were selected within a region of interest, and having T1 error < 2.5 s. With respect to respiratory interventions, only those voxels, which provided consistently reliable data throughout all measurements were included for further analysis. The number of such acceptable voxels ranged from 35 to 150 per tumor. Three consecutive eight minute baseline pO_2 measurements were made in 24 mins, while the rat breathed air (FO_2 = 21%). Four representative animals (one small tumor) also underwent respiratory challenge using 100% O_2 and five pO_2 maps were acquired over 40 mins.

Radiation Experiments

Several hours after the MRI measurements the irradiation study was performed with anesthetized rats breathing air or oxygen and 1.3% isoflurane. The TCD_{50} for the HI tumors was reported to be about 50 Gy (*22*) and we chose a single dose of 30 Gy for irradiation here. The 30 Gy dose was given at a rate of 2 Gy/min using a 6 MeV Siemens KDS linear accelerator. Five rats from the small tumor group and seven from the larger tumor group breathed oxygen 30 min prior to and during irradiation, while the same number

of rats in each group breathed air. To avoid possible artifacts, those four rats used for pO_2 study were part of the group to receive oxygen during irradiation. A treatment plan was designed to irradiate the tumors only and bolus material was used to improve dose uniformity. Control groups without irradiation consisted of six rats each for the small and large tumor groups. Tumor sizes were measured every 3-7 days using a caliper and volume was calculated using the formula: volume = $\pi/6$ abc, where a, b and c are the three respective dimensions. Treatment response was evaluated on the basis of tumor growth delay, which was determined by the time (T_2) required for a tumor to reach two times the treatment volume (V_0).

Markers of vascular endothelium and perfusion

The blue fluorescent dye Hoechst 33342 (Molecular Probes, Eugene, OR) was injected into the tail vein of anesthetized rats at a concentration of 10 mg/kg in 0.9% saline (0.1 ml) and the tumors were excised 1 min later. Tumor specimens were immediately immersed in liquid nitrogen and then stored at -80 °C. Immediately after cryostat sectioning (6 μm thick), slices were imaged for Hoechst 33342 under UV wavelength (330-380 nm). On the following day, the same slices were immunostained for the endothelial marker, CD31. Tissue sections were fixed in acetone for 5 min and then washed in phosphate buffer saline (PBS) for 10 min. A primary mouse anti rat CD31 monoclonal antibody (1:20 dilution; Serotec, Raleigh, NC) was added and incubated for 2 hr at 37 °C in a humid box. Slides were then incubated with horseradish peroxidase (HRP)- conjugated goat anti mouse secondary antibody (1: 50 dilution; Serotec, Raleigh, NC) for 1 hr at 37 °C. After a PBS wash, sections were immersed in the AEC substrate (3-amino-9-ethylcarbazole, Vector Laboratories, Inc., Burlingame, CA) for 15 min at room temperature. Finally, sections were counterstained with hematoxylin and observed under light microscopy. For fluorescent staining, after 2 hr incubation with the primary anti CD31 antibody, slides were incubated with FITC-conjugated goat anti mouse secondary antibody (1:100 dilution; Jackson Immunoresearch Laboratories, West Grove, PA) for 1 hr at 37 °C. After mounting with Vectorshield® medium (Vector Laboratories, Burlingame, CA), the slides were observed under green fluorescence (450-490 nm excitation). Microvascular density (MVD) was evaluated using the 'hot spot' technique described by Weidner *et al.*

(*24*). The five most vascularised areas in each tumor were selected under low-power magnification (4×). MVD was determined by counting the total number of positive CD31 staining cells under high-power magnification (10×; area 0.318 mm^2) and calculating the average number/mm^2.

Statistical Analysis

The statistical significance of changes in oxygenation was assessed using an Analysis of Variance (ANOVA) on the basis of Fisher's Protected Least Significant Difference (PLSD) and the statistical analysis of regression was based on Regression and Bivariate plots (Statview, SAS Inst. Inc., Cary, NC). Kaplan-Meier survival statistics was applied to test the differences in tumor growth delay to two times the initial volume at time of treatment among different groups. Hypoxic fractions ($HF_{5;\,10} < 5$; 10 torr) in all the tumors were calculated from the number of hypoxic voxels in each pO_2 map.

Results

Histology shows that the HI tumor is moderately well-differentiated with uniformly sized tumor cells and pseudoglandular structures. Anti CD31 immunostaining shows extensive distribution of vascular endothelium (Fig. 1a and d) and a mean MVD = 188 ± 11 (se)/mm^2. Comparison of the perfused vessels marked by Hoechst 33342 dye with the vessels immunostained by anti-CD31 in the same region indicated extensive perfusion (Fig. 1a and b) and a good correlation (Fig. 1c).

Overlay of ^{19}F on ^{1}H images (not shown) confirmed that HFB was widely distributed as reported previously (*19*), but predominantly in a central slice. Figure 2 shows typical pO_2 maps of the selected regions obtained from a large tumor with respect to oxygen challenge. While breathing air (baseline) the tumor exhibited extensive hypoxia with 46 of 50 regions (voxels) having pO_2 values less than 10 torr. After 40 min. oxygen inhalation, the initially hypoxic regions became well oxygenated and only one voxel remained hypoxic (~ 5 torr).

Baseline pO_2 distributions obtained from the tumors examined by MRI [four small (363 voxels) and six large (456 voxels) tumors] are presented in Table 1. The small tumors had a mean baseline pO_2 = 29.4 ± 3.2 (se) torr, with a median of 24.6 ± 3.4 torr and mean hypoxic fractions of 10 ± 3 and 20 ± 3% for HF_5 and

HF_{10}, respectively. In comparison, the larger tumors had pO_2 values of mean = 4.6 ± 1.0 torr, median = 2.2 ± 0.8 torr, with HF_5 and HF_{10} of 61 ± 2% and 75 ± 3%, respectively. In agreement with our previous studies (*19, 20*), the larger tumors had a significantly lower mean pO_2 and higher hypoxic fraction ($p < 0.01$) compared with the small tumors. One of the four small and three of the six large tumors were subjected to 40 min. oxygen challenge and dynamic changes in mean pO_2 and hypoxic fraction (HF_{10}) are shown in Table 1 and Fig. 3. Baseline pO_2 (mean = 31.0 ± 2.5 torr; median = 30.0 torr) in the small tumor increased significantly within 8 mins of switching the inspired gas from air to oxygen and reached 179.6 ± 16 torr ($p < 0.0001$; median pO_2 = 177 torr) after 40 mins. All three larger tumors had lower baseline pO_2 (range from 1.3 to 5.2 torr), but increased significantly with a maximum mean for the three = 110.2 ± 13.6 torr; median = 70.1 torr (Table 1 and Fig. 3). One large tumor reached a maximum pO_2 at 24 min, while the other two continued to rise (Fig. 3a). Oxygen breathing significantly reduced the HF_5 from 8 to 2% and HF_{10} from 19% to 4% in the small tumor. In the three larger tumors the HF_5 and HF_{10} were significantly reduced from 62 ± 2% and 77 ± 5% down to 11 ± 5% to 17 ± 7% ($p < 0.01$; Table 1 and Fig. 3b).

Table 2 summarizes tumor growth delay in response to irradiation alone or in combination with oxygen breathing. Sham irradiated small control tumors on rats breathing air needed a mean of 7.2 (median 7) days to reach two times the treatment volume (V_0). Treatment with irradiation alone lengthened the growth period to a mean of 38.8 ± 9.0 days (median = 28 days), and not different compared to the 36.4 ± 6.7 days with irradiation plus oxygen (median = 30 days). For the larger tumors, with radiation alone the T_2 was a mean of 30.9 ± 5.5 days (median = 31 days), compared with a mean of 16.7 ± 1.3 days (median = 16 days) in the control tumors ($p = 0.06$). Rats with large tumors breathing oxygen 30 min prior to and during irradiation yielded an increased T_2 growth delay time of 81.9 ± 14.6 days (median = 77 days). The addition of oxygen produced an enhanced growth delay ratio of 2.7 (81.9/30.9 = 2.7) compared with irradiation alone ($p < 0.01$; Table 2). Individual growth curves for all fourteen larger tumors receiving treatment are plotted in Fig. 4. The Kaplan Meier survival plots (T_2) also showed that oxygen breathing produced an

enhanced growth delay in the larger tumors (Fig. 5). The cumulative survival time for the small tumors (Fig. 5a) truly represents the time each tumor took to reach the T_2 or the time for the tumors to reach two times the initial treatment volume. With the large tumors, depicted in Fig. 5b, the control and air plus irradiation results represent time to reach T_2. In contrast, with the radiation plus oxygen animals, one animal died prior to reaching T_2 and two animals were sacrificed for humane reasons. Thus, with these animals the "T_2" survival time was defined as the time they were removed from the study. We feel justified doing this, since if anything, we are biasing the results toward shorten survival times. Each of these animals lived longer than their irradiation alone contemporaries. Assuming that baseline pO_2 (for air breathing rats) or the maximum pO_2 values observed during oxygen breathing (for IR + O_2) represent the pO_2 values at the time of irradiation, we found a strong linear correlation between the pO_2 values and T_3 (Fig. 6).

Discussion

In this study, we present data which show that the HI tumor, a moderately well-differentiated tumor responds to oxygen breathing by increased pO2 and reduced hypoxia at 5 and 10 torr. These data are in agreement with earlier data and further we show here that smaller tumors (< 2 cm3) are significantly better oxygenated than larger HI tumors (> 3 cm3). This pattern of oxygenation and modulation of oxygen is manifested in their radiation responses. With the small HI tumors a single dose of 30 Gy irradiation caused a significant volume growth delay (~30 days for T_2), but breathing oxygen produced no additional benefit. We believe this reflects baseline oxygenation: while breathing oxygen did essentially eliminate the hypoxic fraction, it started at a very low level (~ 20%), and thus, the tumor cells were already sensitive to irradiation. By contrast, under baseline conditions, larger HI tumors had a substantial hypoxic fraction (HF_{10} = 77%), which was significantly reduced to 17% by breathing oxygen: this resulted in a significant oxygen-enhanced growth delay of about 50 days (T_2; Table 2). Meanwhile, irradiation of large tumors, while rats breathed air, produced no significant growth delay, consistent with the large hypoxic fraction, which would be expected to be radio-resistant. It may be particularly significant that radiation was similarly effective in small or large tumors when the HF_{10} < 20%.

Following Gray's (*25*) demonstration that hypoxic cells are radio-resistant and noting that solid tumors are often hypoxic (*4*), there have been extensive efforts to increase tumor oxygenation (5). Intuitively, one might expect breathing elevated oxygen to improve tumor oxygenation, and hence, enhance response to irradiation. However, some previous investigations have found little or no therapeutic benefit in animals or in the clinic (*9, 26*). Indeed, a meta analysis of 83 clinical trials involving over 10,000 patients showed a modest benefit only, which was restricted to specific tumor types (*3*). As others have speculated, this marginal effect may have resulted from the inability to identify those patients who would benefit from elevated oxygen. As we have seen, irradiation of large HI rat tumors benefited from oxygen inhalation, but the effect would have been masked in a non-stratified population by the small tumors, which showed no effect. Current application of the Eppendorf Histograph provides the capacity to identify hypoxic tumors and some Institutions are incorporating pO_2 measurements into treatment planning. There is increasing clinical evidence that tumor oxygenation is a useful prognostic indicator of patient survival and disease-free survival in cervical cancer (*1, 2*) and head and neck cancer (*10-12*). Initial studies also suggest that the level of hypoxia in breast (*27*), prostate (*28*) and brain (*29*) tumors, may ultimately have prognostic value. There is clearly value in identifying patients with hypoxic tumors, but to identify which patients respond with reduced tumor hypoxia may ultimately be of even greater value.

Generally, pO_2 measurements have been used to assess baseline pO_2 only, but Aquino Parsons *et al.* (*30*) have tested the ability to detect modulation of pO_2 accompanying adjuvant interventions. Repeat Histograph investigations on a group of women with cervical cancer demonstrated improved tumor oxygenation when all subjects breathed carbogen (versus air). Oxygen and carbogen (2.5% or 5% CO_2) were also compared with as many as three series of measurements in each tumor, but of necessity, parallel regions were examined because this approach is highly invasive (*30*). In their study either fraction of CO_2 in the carbogen appeared equally effective. Pure oxygen had little effect on the severely hypoxic fraction < 2.5 torr.

Other studies have shown that the effect of carbogen on radiosensitivity and/or oxygenation appears to be slightly superior to pure oxygen in some tumor types (*31-33*). However, our own previous studies have generally found oxygen and carbogen to have a very similar influence on rat prostate tumor oxygenation irrespective of subline (*e.g.*, Dunning prostate R3327- AT1, HI or MAT-Lu) or size (*18-20*) and agrees well with the recent work published by Thews *et al.*, (*34*). Thews reported no significant differences in oxygenation of an experimental mouse tumor when breathing 100% O_2 compared to 1, 2.5 or 5% $CO_2 + O_2$. Therefore, we elected to test the effect of oxygen on radiotherapy in this current study.

The value of examining dynamic changes is emphasized by reports that efficacy of adjuvant interventions can be influenced by timing, *e.g.*, pre-irradiation breathing time, and indeed, some studies (*33, 35*) have shown that following an initial increase in pO_2, a zenith is reached, followed by a decline. We created pO_2 maps every 8 mins and over a 40 mins breathing time, the mean pO_2 in our HI tumors continually increased and the HF_{10} declined in three of the four tumors (Fig. 3). This is in line with our previous observations using both *FREDOM* and fiber optic probes (*19, 20*).

In common with our previous investigations (*19, 20*), we found that the large Dunning prostate R3327 HI tumors were significantly less well oxygenated than smaller ones: mean and median pO_2 values were lower and hypoxic fraction was greater (Table 1). The representative tumors we used for pO_2 measurement in this study exhibited both baseline pO_2 distribution and response to oxygen inhalation, and not statistically distinguishable from our previous data (*19*). Thus, while both inter- and intra-tumoral heterogeneity were observed, the HI tumors used here showed consistent behavior. This is important since we measured pO_2 in only representative tumors and assumed that other experimental tumors in the groups exhibited similar oxygen distributions and dynamics.

As observed previously (*19, 20*), HI tumors show a remarkable response to oxygen inhalation: even in large tumors the hypoxic fraction < 10 torr (HF_{10}) rapidly decreased from values greater than 60% to as low as 4% (Fig. 3). This must reflect a highly developed vasculature. Indeed, histology showed an extensive vasculature that is well perfused as revealed by the anti CD31 staining (PECAM) and extensive

distribution of Hoechst 33342 dye (Fig. 1). The general histological appearance of the HI tumors is the same as reported by others (*21, 22*).

Others have examined the radio-sensitivity of the Dunning prostate sublines H, HI and AT1 (*22, 36*). Peschke *et al.* (*21, 22*) reported the well-differentiated and less hypoxic H and HI sublines were more sensitive to radiation than the anaplastic AT1, but they did not examine the influence of tumor size.

Dynamic measurements are particularly valuable for assessing the time course of changes with respect to interventions. Historically, single electrodes were applied (*13*) and more recently multiple locations have been interrogated with fiber optic probes (*19, 37*). Dynamic studies using ESR have examined a single location within a tumor (*15, 38*), and permanent sensor implants have permitted chronic studies over hours and days. ESR measurement of pO_2 at a single location has evaluated the time course of hypoxiation and reoxygenation following irradiation of a mouse tumor (*15, 38*). Most significantly, the timing of sequential doses in a two-dose split regimen could be optimized to exploit the observed reoxygenation (*15*).

HFB clears from tumors within 24 h with a $T_{1/2}$ of 600 mins (*39*). This time course allows us to examine acute changes with respect to various interventions ranging from respiratory challenge with inhaled gases, to vasoactive agents (*40*) and vascular targeting drugs (*41*). Short-term changes in pO_2 following irradiation have also been examined (*42*). Other perfluorocarbon reporter molecules show longer tissue residence and we previously used perfluorotributylamine to follow chronic changes during tumor growth over a period of weeks (*43*). The perfluorocarbons administered i.v. sequester in the well perfused regions of the tumor (*44*).

In view of tumor heterogeneity, the general trend among pO_2 measurements has been towards measuring pO_2 distributions and the Eppendorf Histograph is considered by some to be a 'gold standard'. It is the only technique to have widespread clinical applications so far. While it precludes assessment of changes at individual locations within the tumor, strong correlations have been reported between median pO_2 or HF_{10} and surviving fraction based on the clonogenic assay (*45*). We have previously shown that

pO_2 distributions measured using *FREDOM* are not dissimilar from those obtained using the Histograph (*17*). We believe that *FREDOM* could offer an enhanced examination in the future, since needle insertion is required only once and acute dynamic studies can be conducted at multiple individual locations simultaneously. We do, however, recognize that access to clinical ^{19}F MRI is presently limited and costly.

Fyles *et al.* (*2*) had shown that hypoxia in small cervical cancers has little impact on outcome, while it was highly significant for large tumors. More recently, they also reported that the finding is only pertinent to node-negative patients (*46*). Thus, it is reasonable to search for additional prognostic factors other than tumor size (*2*) and recent reports suggest that in certain cases lactate concentration (*47*), apoptosis (*48*), microvascular density (*24*), expression of proteins such as HIF-1 (*49*) or carbonic anhydrase (CA IX) (*50*) could provide additional stratification. Our differentiation of small and large tumors based on the reponse to respiratory intervention agrees with Fyles' report (*2*). Nonetheless, we note that some large HI tumors responded more effectively than others and we are searching for additional parameters to further stratify the tumors.

Since it has been shown that human prostate cancer can have a high hypoxic fraction (*28*), the ability to monitor changes in pO_2 could have important implications in therapeutic strategies. In particular, radiotherapy could benefit from intensity modulated treatment based on loco- regional pO_2.

In conclusion, our results suggest that the ability to detect modulation of tumor pO_2, in particular, the residual hypoxic fraction, with respect to an intervention, could have prognostic value for improving the efficacy of radiotherapy. If the findings we present here are confirmed in prostate cancer patients, it would suggest therapeutic value of monitoring tumor baseline and dynamic pO_2. Tumors like the HI can be modulated and might be expected to show improved response to radiotherapy with oxygen or carbogen inhalation prior to therapy. These results further demonstrate the value of *FREDOM* as a prognostic tool to assess *in vivo* dynamic changes in regional pO_2. We hope our new data showing the predictive value of *FREDOM* with respect to dynamic measurements provides impetus to develop this technique further, *e.g.*,

examine utility in more diverse tumor types, encouraging evaluation in other laboratories and translate measurements to the clinical settings.

Acknowledgments

We are grateful to Drs. Mark Jeffrey and Matthew Merritt for maintaining the MR system, Dr. Kenneth Gall for radiotherapy, Dr. Sophia Ran for valuable advice and discussion for histology, and to Drs. Peter Peschke (DKFZ, Heidelberg) and Peter Antich for ongoing collegial support. Research supported in part by DOD Prostate Cancer Initiative (DAMD 170110108) and NCI RO1 79515.

References

1. M. Höckel, K. Schlenger, B. Aral, M. Mitze, U. Schäffer and P. Vaupel, Association between tumor hypoxia and malignant progression in advanced cancer of the uterine cervix. *Cancer Res.* **56**, 4509-15 (1996).
2. A. W. Fyles, M. Milosevic, R. Wong, M-C. Kavanagh, M. Pintile, A. Sun, W. Chapman, W. Levin, L. Manchul, T. J. Keane and R. P. Hill, Oxygenation predicts radiation response and survival in patients with cervix cancer. *Radiother. Oncol.* **48**, 149-56 (1998).
3. J. Overgaard and M. R. Horsman, Modification of hypoxia-induced radioresistance in tumors by the use of oxygen and sensitizers. *Semin. Radiat. Oncol.* **6**, 10-21 (1996).
4. J. M. Brown, The hypoxic cell: A target for selective cancer therapy-eighteenth Bruce F. Cain memorial award lecture. *Cancer Res.* **59**, 5863-70 (1999).
5. M. Höckel and P. Vaupel, Tumor hypoxia: Definitions and current clinical, biologic, and molecular aspects. *J. Natl. Cancer Inst.* **93**, 266-76 (2001).
6. P. Vaupel, D. K. Kelleher and O. Thews, Modulation of tumor oxygenation. *Int. J. Radiat. Oncol. Biol. Phys.* **42**, 843-8 (1998).
7. A. Rojas, V. K. Hirst, A. S. Calvert and H. J. Johns, Carbogen and nicotinamide as radiosensitizers in a murine mammary carcinoma using conventional and accelerated radiotherapy. *Int. J. Radiat. Oncol. Biol. Phys.* **3**, 357-65 (1996).
8. J. H. A. M. Kaanders, L. A. M. Pop, H. A. M. Marres, I. Bruaset, F. J. A. van den Hoogen, M. A. W. Merkx and A. J. van der Kogel, ARCON: experience in 215 patients with advanced head-and-neck cancer. *Int. J. Radiat. Oncol. Biol. Phys.* **52**, 769-78 (2002).
9. P. Rubin, J. Hanley, H. M. Keys, V. Marcial and L. Brady, Carbogen breathing during radiation therapy: The Radiation Therapy Oncology Group study. *Int. J. Radiat. Oncol. Biol. Phys.* **5**, 1963-70 (1979).

10. D. M. Brizel, G. S. Sibly, L. R. Prosmitz, R. L. Scher and M. W. Dewhirst, Tumor hypoxia adversely affects the prognosis of carcinoma of the head and neck. *Int. J. Radiat. Oncol. Biol. Phys.* **38**, 285-289 (1997).

11. M. Nordsmark, M. Overgaard and J. Overgaard, Pretreatment oxygenation predicts radiation response in advanced squamous cell carcinoma of head and neck. *Radiother. Oncol.* **41**, 31-39 (1996).

12. V. Rudat, B. Vanselow, P. Wollensack, C. Bettscheider, S. Osman-Ahmet, M. J. Eble and A. Dietz, Repeatability and prognostic impact of the pretreatment pO_2 histography in patients with advanced head and neck cancer. *Radiother. Oncol.* **57**, 31-7 (2000).

13. C. W. Song, I. Lee, T. Hasegawa, J. G. Rhee and S. H. Levitt, Increase in pO_2 and radiosensitivity of tumors by Fluosol and carbogen. *Cancer Res.* **47**, 442-446 (1987).

14. J. Bussink, J. H. A. M. Kaanders, A. M. Strik and A. J. van der Kogel, Effects of nicotinamide and carbogen on oxygenation in human tumor xenografts measured with luminescense based fiber-optic probes. *Radiother. Oncol.* **57**, 21-30 (2000).

15. J. A. O' Hara, F. Goda, E. Demidenko and H. M. Swartz, Effect on regrowth delay in a murine tumor of scheduling split-dose irradiation based on direct pO_2 measurements by electron paramagnetic resonance oximetry. *Radiat. Res.* **150**, 549-56 (1998).

16. S. P. Robinson, F. A. Howe, L. M. Rodrigues, M. Stubbs and J. R. Griffiths, Magnetic resonance imaging techniques for monitoring changes in tumor oxygenation and blood flow. *Semin. Radiat. Oncol.* **8**, 198-207 (1998).

17. R. P. Mason, A. Constantinescu, S. Hunjan, D. Le, E. W. Hahn, P. P. Antich, C. Blum and P. Peschke, Regional tumor oxygenation and measurement of dynamic changes. *Radiat. Res.* **152**, 239-49 (1999).

18. S. Hunjan, D. Zhao, A. Constantinescu, E. W. Hahn, P. P. Antich and R. P. Mason, Tumor Oximetry: demonstration of an enhanced dynamic mapping procedure using fluorine-19 echo planar

magnetic resonance imaging in the Dunning prostate R3327-AT1 rat tumor. *Int. J. Radiat. Oncol. Biol. Phys.* **49**, 1097-1108 (2001).

19. D. Zhao, A. Constantinescu, E. W. Hahn and R. P. Mason, Tumor oxygen dynamics with respect to growth and respiratory challenge: Investigation of the Dunning prostate R3327-HI tumor. *Radiat. Res.* **156**, 510-20 (2001).

20. D. Zhao, A. Constantinescu, E. W. Hahn and R. P. Mason, Differential oxygen dynamics in two diverse Dunning prostate R3327 rat tumor sublines (MAT-Lu and HI) with respect to growth and respiratory challenge. *Int. J. Radiat. Oncol. Biol. Phys.* (In press 2002).

21. J. Isaacs, W. Isaacs, W. Feitz and J. Scheres, Establishment and characterization of 7 Dunning prostate cancer cell lines and their use in developing methods for predicting metastatic ability of prostate cancer. *Prostate* **9**, 261-281 (1986).

22. P. Peschke, E. W. Hahn, F. Wenz, F. Lohr, F. Braunschweig, G. Wolber, I. Zuna and M. Wannenmacher, Differential sensitivity of three sublines of the rat Dunning prostate tumor system R3327 to radiation and/or local tumor hyperthermia. *Radiat. Res.* **150**, 423-30 (1998).

23. E. W. Hahn, P. Peschke, R. P. Mason, E. E. Babcock and P. P. Antich, Isolated tumor growth in a surgically formed skin pedicle in the rat: A new tumor model for NMR studies. *Magn. Reson. Imaging* **11**, 1007-1017 (1993).

24. N. Weidner, J. Folkman, F. Pozza, P. Bevilacqua, E. N. Allred and D. H. Moore, Tumor angiogenesis: a new significant and independent prognostic indicator in early-stage breast carcinoma. *J. Natl. Cancer Inst.* **84**, 1875-1887 (1992).

25. L. H. Gray, A. Conger, M. Ebert, S. Hornsey and O. Scott, The concentration of oxygen dissolved in tissues at time of irradiation as a factor in radio-therapy. *Br. J. Radiol* **26**, 638-48 (1953).

26. G. Stuben, M. Stuschke, K. Knuhmann, M. R. Horsman and H. Sack, The effect of combined nicotinamide and carbogen treatments in human tumor xenografts: Oxygenation and tumor control studies. *Radiother. Oncol.* **48**, 143-8 (1998).

27. P. Okunieff, M. Höckel, E. P. Dunphy and P. W. Vaupel, Oxygen tension distributions are sufficient to explain the local response of human breast tumors treated with radiation alone. *Int. J. Radiat. Oncol. Biol. Phys.* **26**, 631-6 (1993).

28. B. Movsas, J. Chapman, E. Horwitz, W. Pinover, R. Greenberg, A. Hanlon, R. Lyer and G. Hanks, Hypoxic regions exist in human prostate carcinoma. *Urology* **53**, 11-8 (1999).

29. R. Rampling, G. Cruickshank, A. D. Lewis, S. A. Fitzsimmons and P. Workman, Direct measurement of pO_2 distribution and bioreductive enzymes in human malignant brain tumors. *Int. J. Radiat. Oncol. Biol. Phys.* **29**, 427-31 (1994).

30. C. Aquino-Parsons, A. Green and A. I. Minchinton, Oxygen tension in primary gynaecological tumours: the influence of carbon dioxide concentration. *Radiother. Oncol.* **57**, 45-51 (2000).

31. J. L. Lanzen, R. D. Braun, A. L. Ong and M. W. Dewhirst, Variability in blood flow and pO_2 in tumors in response to carbogen breathing. *Int. J. Radiat. Oncol. Biol. Phys.* **42**, 855-859 (1998).

32. B. J. P. van der Sanden, A. Heerschap, L. Hoofd, A. W. Simonetti, K. Nicolay, A. van der Toorn, W. N. M. Colier and A. J. van der Kogel, Effect of carbogen breathing on the physiological profile of human glioma xenografts. *Magn. Reson. Med.* **42**, 490-9 (1999).

33. H. D. Suit, N. Marshall and D. Woerner, Oxygen, oxygen plus carbon dioxide, and radiation therapy of a mouse mammary carcinoma. *Cancer* **30**, 1154-1158 (1972).

34. O. Thews, D. K. Kelleher and P. Vaupel, Dynamics of tumor oxygenation and red blood cell flux in response to inspiratory hyperoxia combined with different levels of inspiratory hypercapnia. *Radiother. Oncol.* **62**, 77-85 (2002).

35. S. Falk, R. Ward and N. Bleehen, The influence of carbogen breathing on tumor tissue oxygenation in man evaluated by computerized pO_2 histography. *Br. J. Cancer* **66**, 919-924 (1992).

36. C. Thorndyke, B. Meeker, G. Thomas, W. Laky, M. McPhee and J. Chapman, The radiation sensitivities of R3327-H and -AT1 rat prostate adenocarcinomas. *J. Urol.* **134**, 191-8 (1985).

37. J. Bussink, J. H. A. M. Kaanders, A. M. Strik, B. Vojnovic and A. J. van der Kogel, Optical sensor-based oxygen tension measurements correspond with hypoxia marker binding in three human tumor xenograft lines. *Radiat. Res.* **154**, 547-55 (2000).

38. B. Gallez, B. F. Jordan, C. Baudelet and P. D. Mission, Pharmalogical modification of the partial pressure of oxygen in the murine tumors: Evaluation using in vivo EPR oximetry. *Magn. Reson. Med.* **42**, 627-30 (1999).

39. S. Hunjan, R. P. Mason, A. Constantinescu, P. Peschke, E. W. Hahn and P. P. Antich, Regional tumor oximetry: ^{19}F NMR spectroscopy of hexafluorobenzene. *Int. J. Radiat. Oncol. Biol. Phys.* **40**, 161-71 (1998).

40. D. Zhao, A. Constantinescu, L. Jiang, E. W. Hahn and R. P. Mason, Prognostic radiology: quantitative assessment of tumor oxygen dynamics by MRI. *Am. J. Clin. Oncol.* **24**, 462-6 (2001).

41. R. P. Mason, A. Constantinescu, S. Ran and P. E. Thorpe, Oxygenation in a human tumor xenograft: manipulation through repiratory challenge and antibody directed infarction, In *Oxygen transport to tissue XXII. Proceedings of the 27th annual meeting of the International Society on Oxygen Transport to Tissue*, (J.F. Dunn and H.M. Swartz, Eds), Pabst Verlag, In press 2002.

42. R. P. Mason, S. Hunjan, D. Le, C. Constantinescu, B. R. Barker, P. S. Wong, P. Peschke, E. W. Hahn and P. P. Antich, Regional Tumor Oxygen Tension: Fluorine Echo Planar Imaging of Hexafluorobenzene Reveals Heterogeneity of Dynamics. *Int. J. Radiat. Oncol. Biol. Phys.* **42**, 747-50 (1998).

43. R. P. Mason, P. P. Antich, E. E. Babcock, A. Constantinescu, P. Peschke and E. W. Hahn, Non-invasive determination of tumor oxygen tension and local variation with growth. *Int. J. Radiat. Oncol. Biol. Phys.* **29**, 95-103 (1994).

44. D. J. O. McIntyre, C. L. McCoy and J. R. Griffiths, Tumor oxygenation measurements by ^{19}F MRI of perfluorocarbons. *Curr. Sci.* **76**, 753-762 (1999).

45. D. W. Siemann, I. M. Johansen and M. R. Horsman, Radiobiological hypoxia in the KHT sarcoma: predictions using the Eppendorf Histograph. *Int. J. Radiat. Oncol. Biol. Phys.* **40**, 1171-6 (1998).

46. A. Fyles, M. Milosevic, M. Hedley, M. Pintile, W. Levin, L. Manchul and R. P. Hill, Tumor hypoxia has independent predictor impact only on patients with node-negative cervix cancer. *J. Clin. Oncol.* **20**, 680-7 (2002).

47. S. Walenta, M. Wetterling, M. Leherke, G. Schwichert, K. Sundfør, E. K. Rofstad and W. Mueller-Klieser, High lactate levels predicts likelihood of metastasis, tumor regrowth, and patient survival in human cervix cancers. *Cancer Res.* **60**, 916-27 (2000).

48. M. Höckel, K. Schlenger, S. Höckel and P. Vaupel, Hypoxic cervical cancers with low apoptotic index are highly aggressive. *Cancer Res.* **59**, 4525-28 (1999).

49. H. Zhong, F. Agani, A. A. Baccala, E. Laughner, N. Rioseco-Camacho, W. B. Isaacs, J. W. Simons and G. L. Semenza, Increased expression of hypoxia inducible factor-1 alpha in rat and human prostate cancer. *Cancer Res.* **58**, 5280-5284 (1998).

50. J. A. Loncaster, A. L. Harris, S. E. Davidson, J. P. Logue, R. D. Hunter, C. C. Wycoff, J. Pastorek, R. J. Ratcliffe, I. J. Stratford and C. M. L. West, Carbonic anhydrase (CA IX) expression, a potential new intrinsic marker of hypoxia: Correlation with tumor oxygen measurement and prognosis in locally advanced carcinoma of the cervix. *Cancer Res.* **61**, 6394-99 (2001).

Legends

Fig. 1 Immunohistochemical comparison of perfused vessels marked by Hoechst dye 33342 and total vessels detected by anti CD31. a) Fluorescent image showing extensive distribution of vascular endothelium (green) in a representative large HI tumor (4.5 cm^3). b) The perfused blood vessels marked by blue Hoechst dye in the same region. c) Superposition of the b) on a) showing a good overlap between the total vessels (anti CD31) and the perfused vessels (Hoechst dye). d) Light microscopic image showing distribution of vascular endothelium stained by anti CD31 (pink).

Fig.2 pO_2 maps obtained using the *FREDOM* approach from a representative large Dunning prostate R3327-HI tumor (9.5 cm^3). a) Third baseline map (breathing air: FO_2 = 21%): mean $pO_2 = 2.8 \pm 0.7$ (SE) torr, median $pO_2 = 3.0$ torr (range 0.1 to 13.0 torr). b) Breathing oxygen (FO_2 = 100%): 5th map obtained 32 - 40 minutes after switching from air: mean $pO_2 = 135.3 \pm 11.9$ torr ($p < 0.0001$ compared to baseline), median $pO_2 = 109.9$ torr (range 5.2 to 498 torr). Dynamic data shown as open circle in Fig. 3.

Fig. 3 Dynamic oxygenation and hypoxic fraction in response to respiratory challenge. a) Mean ± SE pO_2 obtained from sequential maps of one small (solid) and three larger HI (open) tumors with respect to respiratory challenge. * $p < 0.001$, ** $p < 0.0001$ compared to mean baseline. b) Corresponding hypoxic fraction (HF_{10}) in these tumors (same symbol) decreased dramatically in response to oxygen breathing.

Fig. 4 Individual normalized tumor volumes in response to irradiation alone (n = 7; solid) or in combination with oxygen breathing (n = 7; open) in the larger tumors. Tumors were treated by 30 Gy irradiation on day 0. One large tumor (dotted line) in the oxygen breathing group died after 77 days with obviously shrunken tumor size: T_2 for this tumor was considered to be 77 days.

Fig. 5 The Kaplan Meier survival plots indicate time to reach 2 x initial size (T_2). a) For small tumors, significant growth delays were observed in irradiated tumors compared with sham irradiated control tumors ($p < 0.01$), but oxygen breathing did not show additional beneficial effect. b) By contrast, a significant growth delay (51 days; $p < 0.01$) was observed in large HI tumors when rats breathed oxygen 30 min prior to and during irradiation.

Fig. 6 Estimated pO_2 values at time of irradiation versus T_2 showed strong correlation ($R = 0.9$). The trendline is plotted excluding the small tumor with oxygen breathing (*). Irradiation alone (triangle) or with oxygen breathing (circle), 3 small (filled) and 6 larger (open) tumors.

Table 1 pO_2 measurements and outcome of irradiation

Group	Rat no.	Baseline breathing air (21% O_2)				Oxygen challenge (100% O_2)				Outcome	
		pO_2 (torr)		HF_5	HF_{10}	pO_2 (torr)		HF_5	HF_{10}	Treatment	T_2
		Mean$^+$ ± SE	Median$^+$	Mean$^+$ ± SE (%)		Mean ± SE	Median	Minimum (%)			(days)
Small (< 2 cm^3)	1	21.7 ± 1.3	16.2	14 ± 4	26 ± 5	NA	NA	NA	NA	30 Gy	20
	2	28.1 ± 1.5	22.0	13 ± 1	20 ± 2	NA	NA	NA	NA	30 Gy	25
	3	31.0 ± 2.5	30.0	8 ± 2	19 ± 2	179.6 ± 16.0*	177.4	2	4	30 Gy + O_2	23
	4	37.0 ± 1.5	30.1	3 ± 1	14 ± 2	NA	NA	NA	NA	30 Gy + O_2	47
	Mean	29.4 ± 3.2	24.6 ± 3.4	10 ± 3	20 ± 3						29
Large (> 3.5 cm^3)	5	4.3 ± 1.2	2.0	62 ± 7	74 ± 10	NA	NA		NA	30 Gy	15
	6	8.8 ± 0.9	5.1	50 ± 7	67 ± 5	NA	NA		NA	30 Gy	16
	7	3.8 ± 0.7	1.3	66 ± 3	80 ± 4	NA	NA		NA	30 Gy	38
	Mean	5.6 ± 1.6‡	2.8 ± 1.2‡	59 ± 5‡	74 ± 4‡						23
	8	1.3 ± 1.1	0.1	65 ± 3	80 ± 5	106.7 ± 13.6*	70.1	15	22	30 Gy + O_2	55
	9	5.2 ± 1.2	0.9	60 ± 7	67 ± 10	88.5 ± 16.5*	53.9	17	26	30 Gy + O_2	57
	10	4.0 ± 0.9	4.0	61 ± 5	84 ± 6	135.3 ± 11.9*	109.9	1	4	30 Gy + O_2	118
	Mean	3.5 ± 1.2‡	1.7 ± 1.2‡	62 ± 2‡	77 ± 5‡	110.3 ± 13.3*	78 ± 18.6	11 ± 5*	17 ± 7*		77

$^+$ values represent the mean values across the 3 baseline observations; T_2: time to 2 times initial volume (V_0); * $p < 0.01$ from baseline;

‡ $p < 0.01$ from the small tumors; HF_5 or $_{10}$: Hypoxic fraction (< 5 or 10 torr); HF_5 or $_{10}$ Minimum: minimum value among the five measurements with respect to oxygen breathing; NA: not measured.

Table 2 Tumor growth delay in response to irradiation alone or combined with oxygen breathing

	Treatment	No.	V_0 (cm^3) Mean ± SE	T_2 (days) Mean ± SE	T_2 (days) Median	Tumor growth delay ratio
Small (< 2 cm^3)	control (air)	6	1.2 ± 0.2	7.2 ± 0.7	7	
	30 Gy	5	1.4 ± 0.2	38.8 ± 9.0*	28	0.9
	30 Gy + O_2	5	1.7 ± 0.4	36.4 ± 6.7*	30	
Large (> 3.5 cm^3)	control	6	4.3 ± 0.2	16.7 ± 1.3	16	
	30 Gy	7	6.7 ± 1.3	30.9 ± 5.5	31	2.7
	30 Gy + O_2	7	7.9 ± 1.3	81.9 ± 14.6+‡	77	

V_0: initial tumor volume; T_2: time to 2 times V_0. * $p < 0.01$ from control group in the small tumors; + $p < 0.001$ from control group and ‡ $p < 0.01$ from irradiation alone group in the large tumors.

Fig. 1

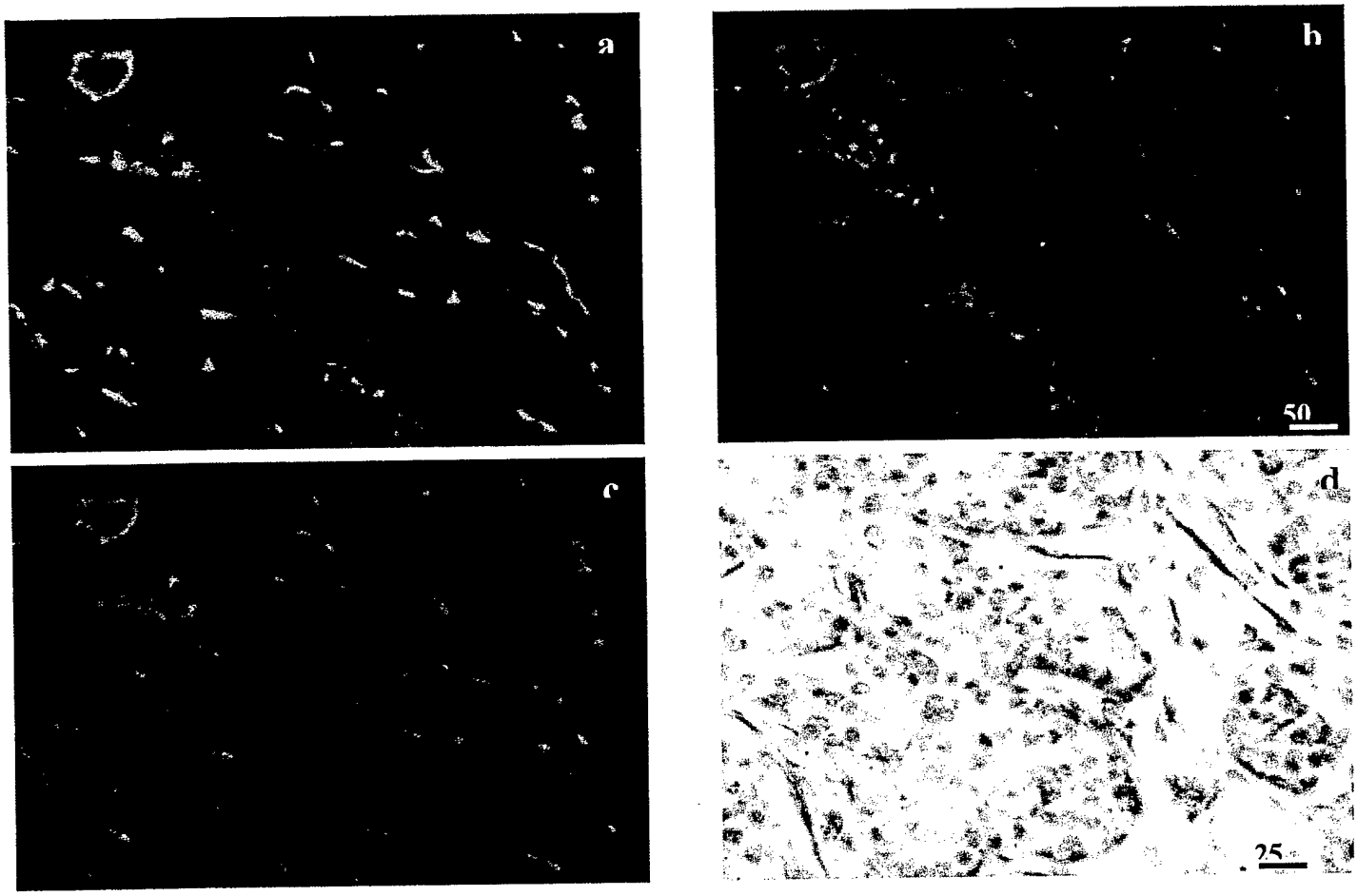

Fig. 2

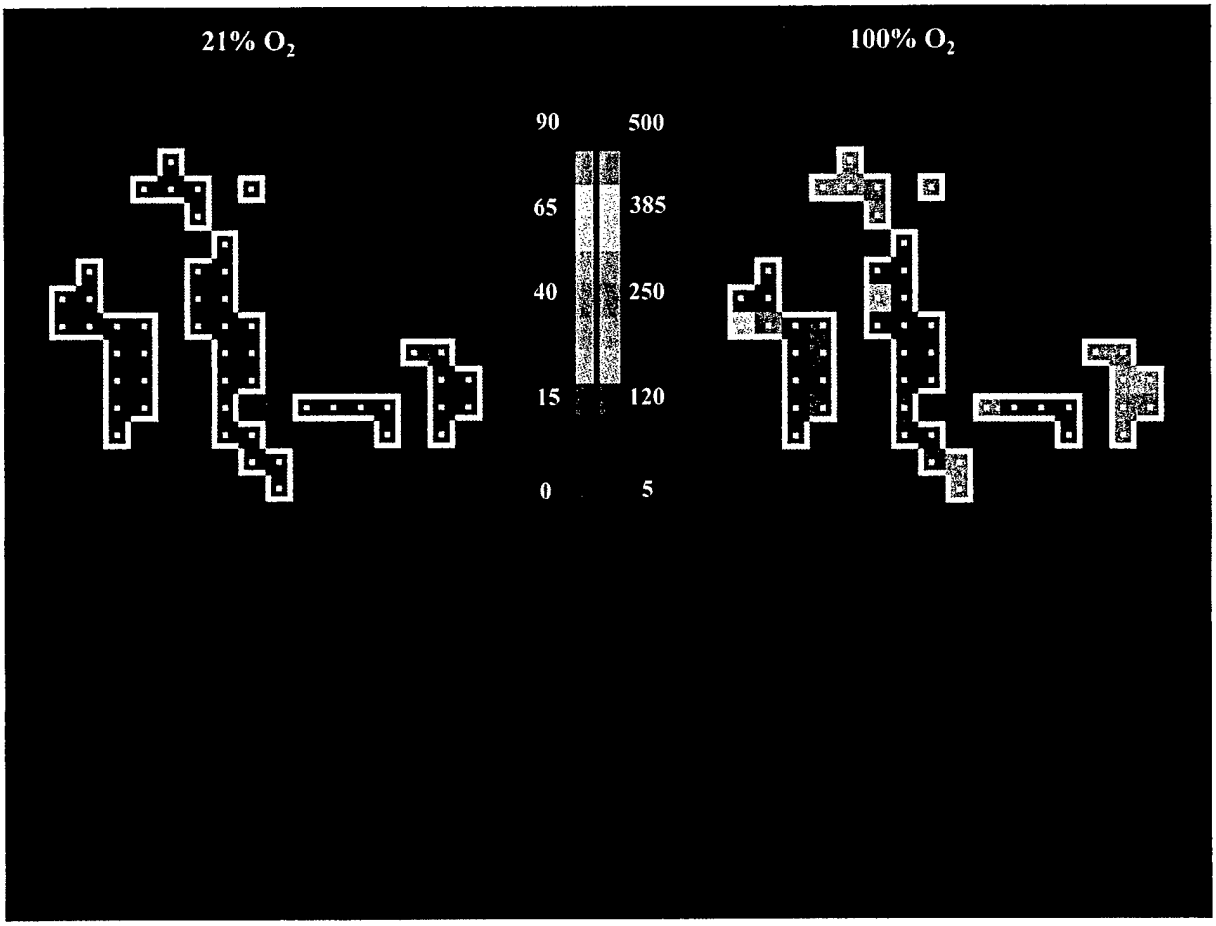

Fig. 4

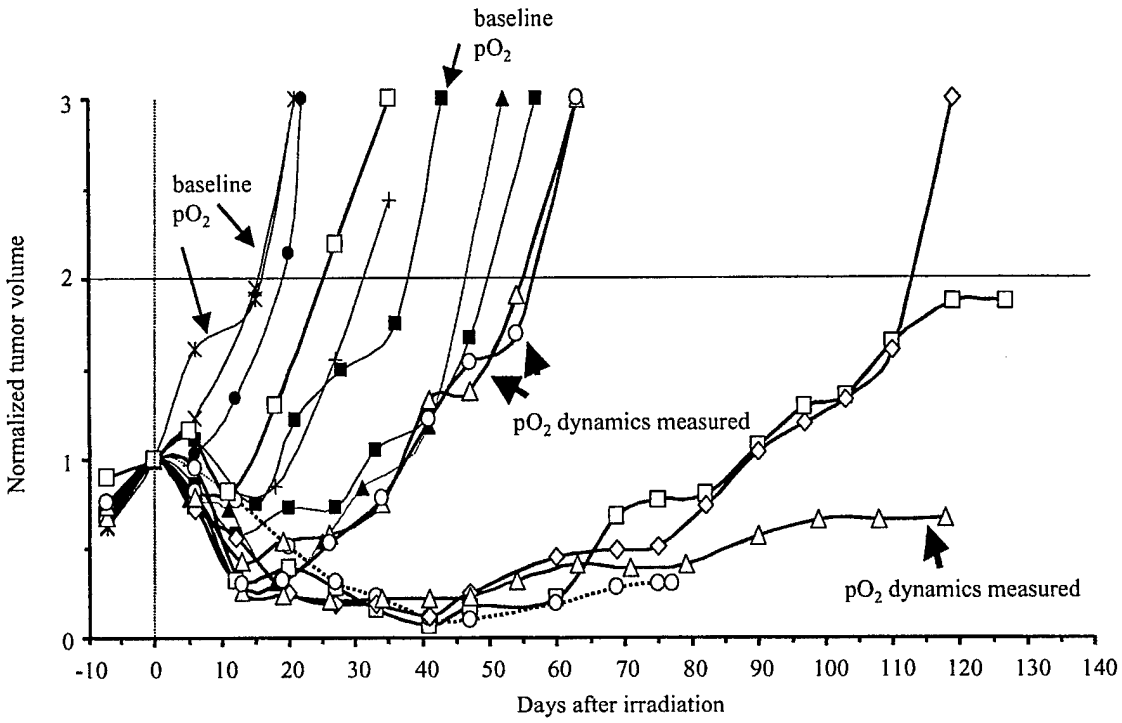
baseline
pO_2
baseline
pO_2
pO_2 dynamics measured
pO_2 dynamics measured
Normalized tumor volume
Days after irradiation
0
1
2
3
-10
0
10
20
30
40
50
60
70
80
90
100
110
120
130
140

Fig. 5

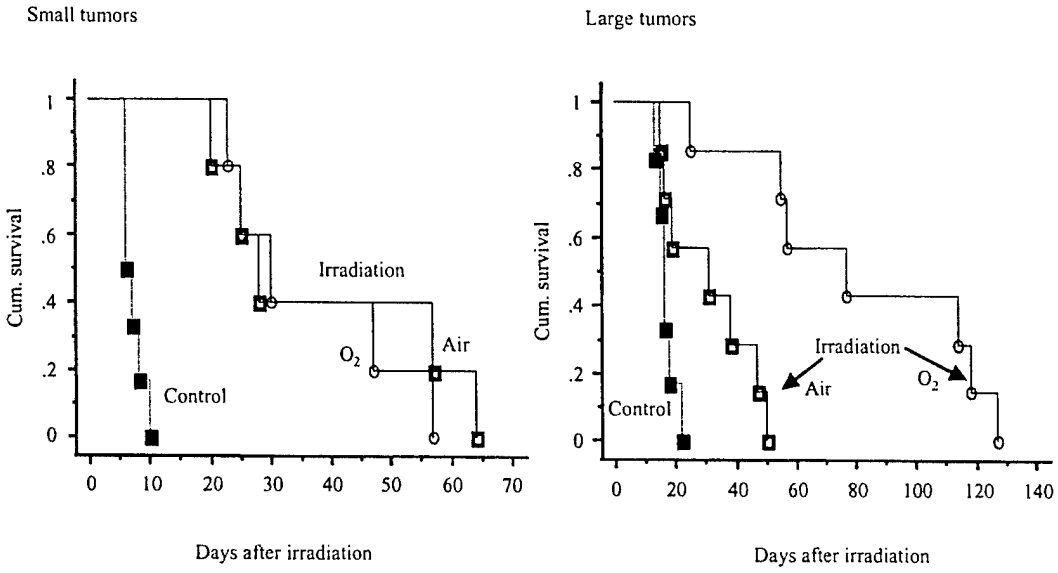
Small tumors
Large tumors
Cum. survival
1
.8
.6
.4
.2
0
Irradiation
O_2
Air
Control
0
10
20
30
40
50
60
70
Days after irradiation
Cum. survival
1
.8
.6
.4
.2
0
Irradiation
Air
O_2
Control
0
20
40
60
80
100
120
140
Days after irradiation

Fig. 6

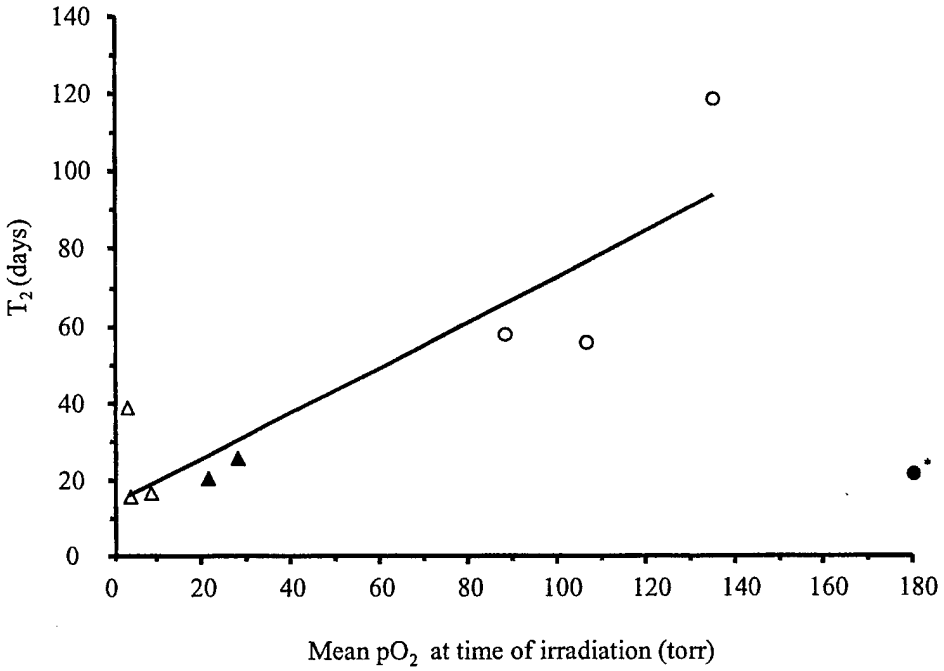
140
120
100
80
60
40
20
0
T_2 (days)
0
20
40
60
80
100
120
140
160
180
Mean pO_2 at time of irradiation (torr)

PROCEEDINGS

New Discoveries in Prostate Cancer Biology and Treatment

December 5-9, 2001
The Registry Resort
Naples, Florida

Conference Co-Chairpersons

KENNETH J. PIENTA
University of Michigan
Comprehensive Cancer Center
Ann Arbor, MI

ROBERT H. GETZENBERG
University of Pittsburgh
Pittsburgh, PA

DONALD S. COFFEY
Johns Hopkins Hospital
Baltimore, MD

In vivo MRI monitoring of prostate tumor vasculature and oxygen dynamics

Dawen Zhao, Lan Jiang, Anca Constantinescu, Eric W. Hahn and Ralph P. Mason, Department of Radiology, U.T. Southwestern Medical Center, Dallas, TX 75390.

Hypoxic cells in solid tumors, has long been recognized as a significant factor influencing response to cancer therapy and prognosis. We recently established a novel magnetic resonance approach to measuring regional tumor oxygen tension: *FREDOM* (Fluorocarbon Relaxometry using Echo planar imaging for Dynamic Oxygen Mapping) using hexafluorobenzene, as the reporter molecule (1, 2). Recognizing the intimate interplay of tumor oxygenation and blood flow, we began investigations to compare regional changes in pO_2, vascular oxygenation and blood flow. Here, we compare perfusion and oxygen dynamics in two Dunning R3327 prostate rat tumor sublines (3): the well differentiated slower growing H subline (Tpot ~ 20 days) and the anaplastic faster growing AT1 subline (Tpot ~ 4.6 days). MRI experiments were performed on a 4.7 T MR system. Vascular oxygen dynamics were assessed using BOLD (Blood Oxygen Level Dependant) contrast ^1H MRI. A series of echo planar images was acquired, while the rat breathed air and in response to respiratory challenge with oxygen (1 dm^3/min). Differences in signal intensity enhancement in response to oxygen inhalation were found between the H (40%) and the AT1 (25%) tumors ($p<0.05$). Increased signal may be interpreted as increased HbO_2. Following a re-equilibration period, dynamic Gd-DTPA contrast-enhanced (DCE) MRI was performed using a spin-echo T1-weighted pulse sequence. The data also revealed significantly higher signal enhancement in H (38%) compared to AT1 (15%) tumors ($p<0.05$). Finally, *FREDOM* performed on the same 4 mm thick tumor section revealed considerable intra tumoral heterogeneity in the distribution of pO_2 values. H tumors had a higher mean baseline pO_2 (30.5 ± 1.6 mmHg) than size-matched AT1 (13.6 ± 0.5 mmHg) tumors ($p<0.001$). Further, although both tumor types responded to respiratory challenge, oxygen inhalation produced a significantly higher maximum pO_2 ($p<0.001$) in H (121.6 ± 6.8 mmHg) compared with AT1 (58.3 ± 3.8 mmHg) tumors. Immunohistochemical studies using the hypoxic marker (pimonidazole) and the vascular endothelial cell marker (CD31) verified that the H subline with 2% positive pimonidazole binding is better oxygenated than the AT1 subline (11%), and vascular density is also higher in H than AT1 tumors. In summary, we believe that the BOLD and DCE MRI, which provide a qualitative index of vascular oxygenation and flow, when combined with quantitative data on tissue oxygenation by ^{19}F MR provide valuable insight into tumor physiology, specifically related to the proficiency of the vascular component and is relevant to treatment response and prognosis. References: 1. Hunjan, S., Zhao, D., Constantinescu, A., Hahn, E. W., Antich, P. P., and Mason, R. P. Int. J. Radiat. Oncol. Biol. Phys. 49, 1097-1108, 2001. 2. Zhao, D., Constantinescu, A., Hahn, E. W., and Mason, R. P. Radiat. Res. 157, in the press 2002. 3. Isaacs, J., Isaacs, W., Feitz, W., and Scheres, J. Prostate 9, 261-81, 1986. (Supported by the DOD Prostate Cancer Initiative (DAMD 170110108) and NCI RO1 79515)

FINAL PROGRAM

FOURTH INTERNATIONAL SYMPOSIUM ON ANTI-ANGIOGENIC AGENTS

Recent Advances and Future Directions in Cell Biology and Clinical Research

The Adam's Mark Hotel **Dallas, Texas**

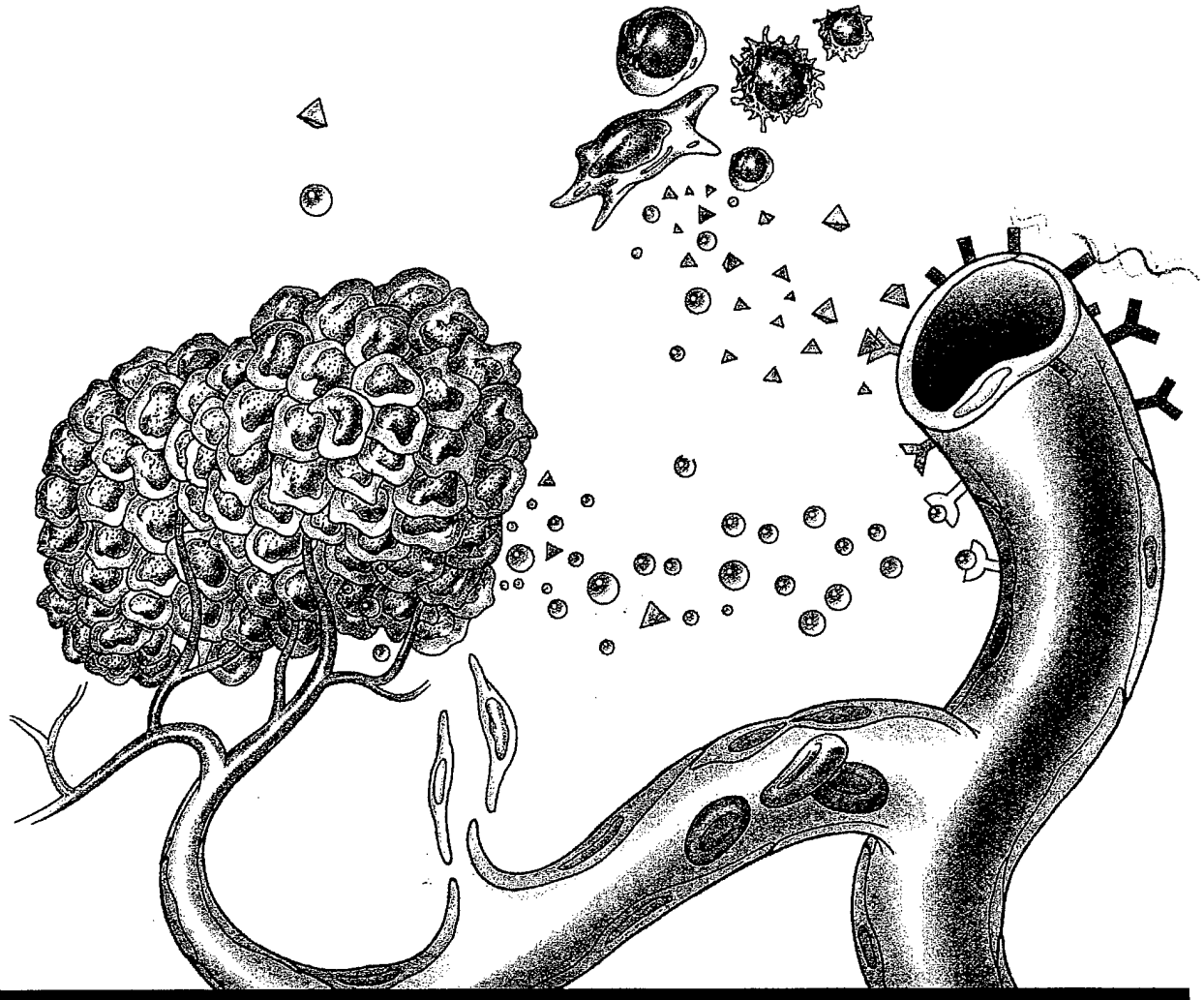

Co-Chairmen

Michael S. Gordon, MD
University of Arizona College of Medicine

George W. Sledge, Jr., MD
Indiana University School of Medicine

Lee M. Ellis, MD
The University of Texas
M.D. Anderson Cancer Center

Robert S. Kerbel, PhD
Sunnybrook and Women's College
Health Sciences Center
University of Toronto

James M. Pluda, MD
National Cancer Institute

SPONSORED BY

CBCE
The Center for Biomedical Continuing Education

In vivo MRI monitoring of tumor oxygen dynamics and correlation with histological findings

Dawen Zhao*, Sophia Ran+, Anca Constantinescu*, Eric W. Hahn* and Ralph P. Mason*

Departments of Radiology* and Pharmacology+, U.T. Southwestern Medical Center, Dallas, TX

Tumor oxygenation status has long been recognized as a significant factor influencing anticancer therapy. Hypoxia in solid tumors, resulting in part from inadequate blood supply, stimulates tumor angiogenesis. A major program in our laboratory is to understand basic physiological mechanisms in tumors by using tumors having different growth rates and histology. Here, we compare oxygen dynamics in two Dunning prostate R3327 rat tumor sublines: the well differentiated slower growing H subline (Tpot 16 days) and the anaplastic faster growing AT1 subline (Tpot 5 days). We used *FREDOM* (Fluorocarbon Relaxometry using Echo planar imaging for Dynamic Oxygen Mapping) with hexafluorobenzene, as the reporter molecule to measure regional tumor oxygen tension using a 4.7 T MR system. *FREDOM* revealed considerable intra tumoral heterogeneity in the distribution of pO_2 values. H tumors had a higher mean baseline pO_2 (12.7 ± 1.1 mmHg) than size-matched AT1 (3.9 ± 1.5 mmHg) tumors ($p<0.001$). Immunohistochemical studies using the hypoxic marker pimonidazole and the vascular endothelial cell marker CD31 verified that the H subline with 2% positive pimonidazole binding is better oxygenated than the AT1 subline (11%), and microvascular density (MVD) is also higher in H than AT1 tumors. Moreover, the co-localization of HIF-1α and VEGF found in the H tumor cells supports the evidence that hypoxia upregulates the expression of VEGF.

In summary, these results concur with the hypothesis that the level of hypoxia is related to tumor growth rate and in turn to the level of vascular differentiation and suggest a non-invasive approach to assessing vascular development.

Supported by the DOD Prostate Cancer Initiative (DAMD 170110108) and NCI RO1 79515.

PROGRAM & ABSTRACTS

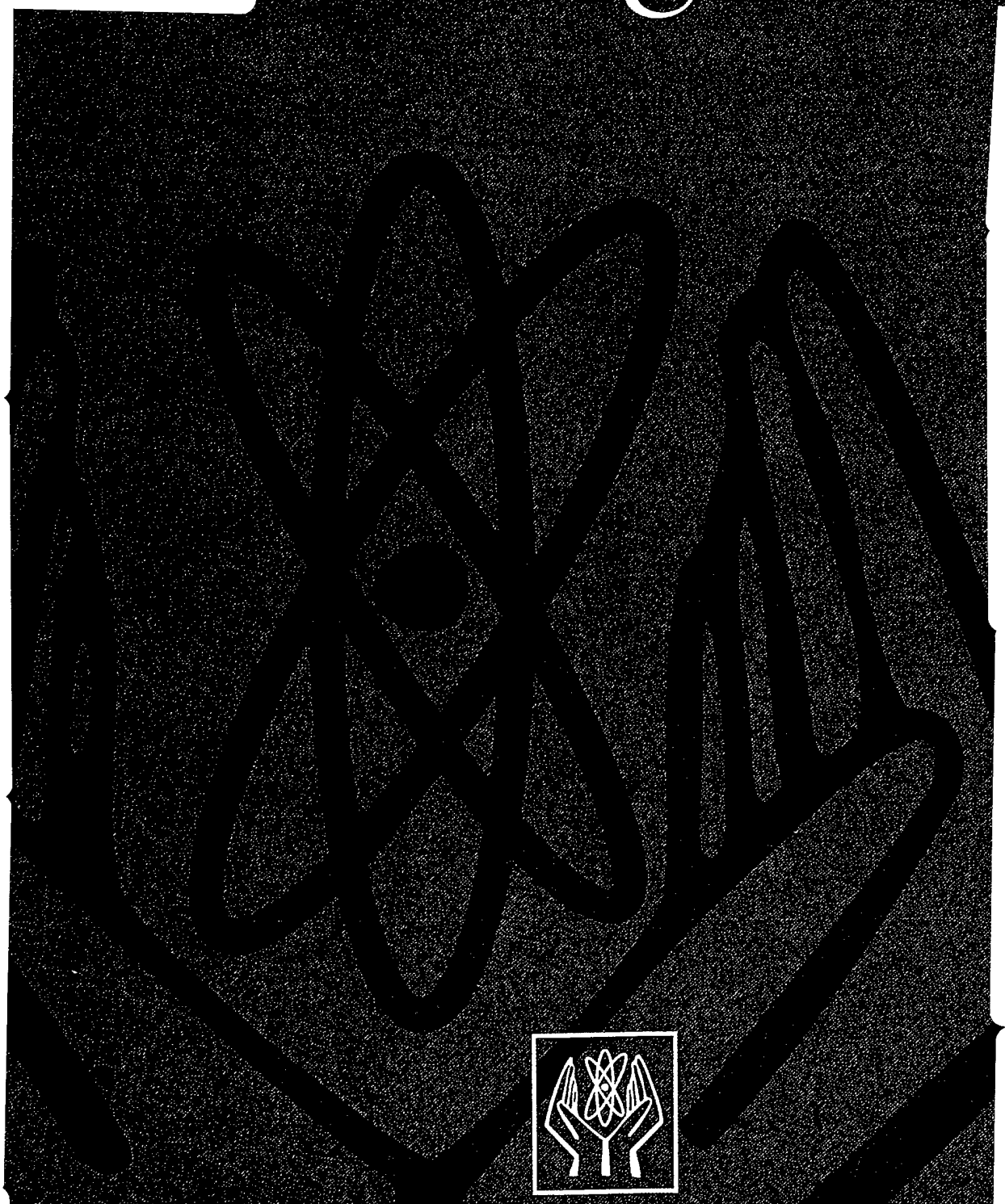

Forty-ninth Annual Meeting of the
Radiation Research Society

and the

Twentieth Annual Meeting of the
North American Hyperthermia Society

April 20–April 24, 2002
Reno Hilton
Reno, Nevada

In Joint Sponsorship with the
Radiological Society
of North America

pump). Each tumor-bearing rat was placed under continuous gas anesthesia, using air + ~ 2% Isoflurane, then administered EF5 at -3 hr before X-ray at time '0'. At -40 min. DDFP or saline was administered over 30 min. at 23 microliter/min. At -10 min., the anesthetic gas was either continued with air (for controls) or switched to carbogen (95% O2 + 5% CO2). The tumor was then irradiated and processed for evaluation of radiation response by an *in vivo-in vitro* assay. The EF5 binding period was used to quantify the pre-existing level of tumor hypoxia. The animals were only subjected to carbogen for the last few minutes of the 3 hr EF5 drug exposure, at the time of irradiation. Carbogen alone provided only minimal sensitization. Similarly, DDFP treatment with air was not different than controls without drug. However, DDFP plus carbogen caused dramatic sensitization, and has provided a highly significant decrease in surviving fraction. The response for tumors in the DDFP + carbogen group was the same as for Morris 7777 cells irradiated in air after disaggregation from the tumor, e.g. a completely aerobic radiation response. DDFP plus carbogen appears to completely reverse the hypoxic cell radioresistance in this tumor model. To our knowledge, no previous study has achieved such a complete elimination of radioresistance. For example, misonidazole and etanidazole have only been useful for providing modest sensitization of very radioresistant tumors, and would not provide any sensitization to tumors of intermediate hypoxia.

(P10-86) Hypoxia Marker Binding Predicts for Outcome in Cancer of the Cervix. C. Aquino-Parsons[1], J.P. Banath[1,*], J.A. Raleigh[2,*] and P.L. Olive[1,*]. [1]British Columbia Cancer Agency, 600 W. 10th Ave., Vancouver, B.C. V5Z 1L3. [2]University of North Carolina, Chapel Hill, NC 27599.

Low tumor oxygenation measured using oxygen microelectrodes is known to be predictive for poor outcome in cancer of the cervix. To determine whether the hypoxia marker, pimonidazole, would show a similar predictive ability, patients with invasive epithelial cervical cancers, FIGO stages Ib to IVa, were given pimonidazole hydrochloride as an i.v. infusion (0.5 gm/m^2) 24 hours before tumor biopsy. Patients were subsequently treated with the current standard course of radiation and weekly cisplatinum. After incisional biopsy, a single cell suspension was prepared from approximately 100 mg tumor, and cells were fixed in 70% ethanol. Flow analysis of these samples was performed using anti-pimonidazole antibody, and histograms were analyzed using a curve fitting program that defined hypoxic cells as those that bound on average 10 times more pimonidazole antibody than the well-oxygenated cells of the tumor. In 68 tumor biopsies analyzed for pimonidazole binding, the percentage of hypoxic cells ranged from 0 to 23% with a mean of 5.9%. In 45 patients where follow-up time has now exceeded 1 year, none of the 8 patients with tumors containing less than 1.5% hypoxic cells has yet shown evidence of disease. However, local recurrence and/or metastases were observed in 25% of the remaining 37 patients. These results support the use of hypoxia markers to identify patients with cervical cancer that will respond well to treatment.

(P10-87) Comparison of hypoxia and microvascular density in the slow growing well differentiated H vs. the faster growing anaplastic AT1 Dunning Prostate R3327 rat tumor. D. Zhao[1,*], E.W. Hahn[1,*], S. Ran[2], A. Constantinescu[1] and R.P. Mason[1,*]. [1]Department of Radiology, U.T. Southwestern Medical Center, Dallas, TX 75390. [2]Department of Pharmacology, U.T. Southwestern Medical Center, Dallas, TX 75390.

Tumor oxygenation status is recognized as a significant factor influencing the outcome of radiation therapy. A major program in our laboratory is to understand basic physiological mechanisms that are associated with the level of hypoxia in tumors, by using tumors having diverse growth rates and histology. Here, we compare oxygen dynamics in two Dunning prostate R3327 rat tumor sublines: the well differentiated slower growing H subline (Tpot 16 days) and the anaplastic faster growing AT1 subline (Tpot 5 days). The tumors were transplanted to surgically formed skin pedicles located on the foreback of adult male Copenhagen rats and examined when they were 2~3 cm diameter. We used *FREDOM* (Fluorocarbon Relaxometry using Echo planar imaging for Dynamic Oxygen Mapping) with hexafluorobenzene, injected intratumorally, as the reporter molecule to measure regional tumor oxygen tension using a 4.7 T MR system. We also carried out immunohistochemical studies using pimonidazole to determine the level and distribution of hypoxia and the vascular endothelial cell marker CD31 to determine the micro-vascular density. As expected, *FREDOM* revealed considerable intra tumoral heterogeneity in the distribution of pO_2 values. H tumors had a higher mean baseline pO_2 (12.7 ± 1.1 mmHg) than size-matched AT1 (3.9 ± 1.5 mmHg) tumors ($p<0.001$). The HF<10 mmHg was 45.7 ± 4.8 percent in the H tumors compared to 83.2 ± 3.5 per cent for the AT1 tumors ($p<0.001$). Two percent of the tumor cells in the H tumors were bound with pimonidazole compared to the AT1 subline in which 11% of the cells were pimonidazole positive. Microvascular density (MVD) was also higher in H vs. AT1 tumors. In summary, these results concur with our working hypothesis that the level of hypoxia is related to tumor growth rate and in turn to the vascular architecture. Supported by the DOD Prostate Cancer Initiative (DAMD 170110108) and NCI RO1 79515.

(P10-88) Comparison of the Comet Assay and Eppendorf Electrode to Measure Tumor Oxygenation in Head and Neck Cancer Patients. M.J. Dorie[1,*], D. Terris[2,*], H. Pinto[3], D. Bloch[4], Q.T. Le[1], J.M. Brown[1,*] and M.S. Kovacs[1,*]. [1]Department of Radiation Oncology, Stanford University, Stanford, CA 94305. [2]Department of Surgery, Stanford University, Stanford, CA 94305. [3]Department of Medicine, Stanford University, Stanford, CA 94305. [4]Department of Health Research and Policy, Stanford University, Stanford, CA 94305.

As part of a clinical trial of the addition of tirapazamine to chemoradiotherapy of node positive stage IV head and neck cancer, we measured the oxygenation of the neck nodes prior to treatment using both the Eppendorf oxygen electrode and the induction of DNA single strand breaks (SSBs) after a dose of 5 Gy using the alkali comet assay. The median oxygenation (by Eppendorf) was 11.8 mmHg for the tumors and 51.9 mmHg for the normal subcutaneous tissue. In addition to fine needle aspirates taken 1, 2 and 3 minutes after the 5 Gy dose, we took samples prior to irradiation to establish a baseline comet tail moment, and irradiated these samples *in vitro* to establish the tail moment distribution in fully oxygenated cells following 5 Gy. We analyzed the comet distributions using median tail moment (MTM) after removal of baseline contamination due to the presence of unirradiated cells in the sample. We found a highly significant correlation between the MTM values for 1 and 2 minutes ($r^2=0.66$, $p<0.0001$) thereby demonstrating the reliability of the assay. The slope of this line is consistent with the expected half-life of 3 minutes for the repair of radiation-induced SSBs. A comparison of the *in vivo* and *in vitro* MTM data indicates that the inter-tumor variation in DNA damage is not due to differences in intrinsic radiosensitivity between tumors, but rather due to variation in oxygenation from tumor to tumor. However, we found no correlation between the Eppendorf median pO_2 and the comet MTM ($r^2=0.09$). The data for tumor oxygenation determined by the comet assay and clinical outcome will be presented.

(P10-89) Tumor hypoxia assessment in breast cancer. M.A. Varia[1,*], S.C. Chou[1], C.A. Ballenger[2], S. Maygarden[3], L. Licht[1] and J.A. Raleigh[1,*]. [1]Department of Radiation Oncology, Universityof North Carolina, Chapel Hill, NC 27599. [2]Department of Radiation Oncology, Duke University Medical Center, Durahm, NC 27710. [3]Department of Pathology, University of North Carolina, Chapel Hill, NC 27599.

As tumor hypoxia predicts for poor prognoses in human cancers, there is increasing interest in developing methods of hypoxia assessment. Several clinical studies show the presence of tumor hypoxia in uterine cervical carcinoma, head and neck cancer, and soft tissue sarcomas, however little is known about the presence of tumor hypoxia in breast cancer, the most common cancer in women. We have initiated studies of tumor hypoxia assessment in human breast cancer using pimonidazole as the hypoxia marker. Patients with biopsy confirmed breast carcinoma are enrolled in two Institutional Review Board studies of tumor hypoxia assessment after informed consent is obtained. Thirty-seven patients were infused with pimonidazole hydrochloride in saline at a dose

radiotherapy in Dunning prostate R3327-HI tumors

D. Zhao, A. Constantinescu, K.C. Chang, K. Gall, E.W. Hahn, and R.P. Mason,
Departments of Radiology and Radiation Oncology, U.T. Southwestern Medical Center, Dallas, TX, USA

It is generally recognized that accurate measurement of tumor ɔygenation could predict response to radiotherapy. We have recently ıtablished a magnetic resonance approach to measuring regional ımor oxygen tension *FREDOM* (Fluorocarbon Relaxometry using cho planar imaging for Dynamic Oxygen Mapping) with ɔxafluorobenzene, as a reporter molecule. *FREDOM* data showed at the hypoxic fraction in large Dunning prostate R3327-HI tumors ɔcreased significantly with oxygen inhalation. Here, we tested the ffect of the adjuvant intervention of oxygen inhalation on diotherapy of these tumors. Radiation induced growth delay ıresponded with decreased hypoxic fraction.

Introduction: It is recognized that tumor hypoxia ıfluences the outcome of radiation therapy, and ıcreased tumor oxygenation promotes radiosensitivity. /e have developed a method to measure tumor oxygen ınsion quantitatively and now demonstrate its prognostic alue with respect to radiation induced tumor growth ɔlay. The *FREDOM* approach exploits the strong ɔnsitivity of the ^{19}F NMR spin lattice relaxation rate of ıe reporter molecule hexafluorobenzene to pO_2 (1). Our ırlier studies showed that oxygen inhalation gnificantly decreased tumor hypoxia in the moderately ell differentiated subline of Dunning prostate R3327-HI ıt carcinoma (2). To test our hypothesis that oxygen ıhalation is an effective adjuvant intervention for ıdiotherapy, we compared tumor response to ionizing ıdiation alone or in combination with oxygen inhalation.

Methods: Syngeneic Dunning prostate R3327-HI ımors (moderately well differentiated, volume doubling me 9 days; TCD_{50} ~ 50 Gy) were implanted in surgically ɔrmed skin pedicles on the foreback of male openhagen rats. Tumors were measured thrice weekly ith calipers. Tumors were allowed to grow to ~1 cm iameter (~0.6 cm^3) or 2 cm diameter (> 3.5 cm^3), at hich time they were divided into groups for irradiation. rior to irradiation, pO_2 was assessed in selected tumors sing *FREDOM*. Hexafluorobenzene (50 µl) was injected irectly into the tumor. A size matched $^1H/^{19}F$ single turn ɔlenoid coil was placed around the tumor and MR ɔperiments were performed using a 4.7 T magnet with ctively shielded gradients. Tumor oxygenation was ɜssessed using ^{19}F PBSR-EPI of HFB with 8 minute time ɔsolution. For those rats, which would breathe oxygen ıring irradiation, a respiratory challenge with oxygen ɔas performed to assess the response of tumor pO_2. egional pO_2 was estimated using the relationship: pO_2 ɔrr) = (R1-0.0835)/0.001876.

Several hours after MRI measurements, irradiation ɔas performed using a single dose (30 Gy) at 6 MeV on a iemens KDS linear accelerator. Half the rats breathed xygen for 30 min prior to and during irradiation, while ıe others breathed air. A treatment plan was designed to radiate the tumors only and bolus material was used to nprove dose uniformity.

Results: In common with our previous findings (2), the ırger tumors (> 3.5 cm^3) exhibited greater hypoxia than the smaller tumors (< 2 cm^3). Baseline mean and median pO_2 were 28.4 ± 1.1 torr and 25.3 torr in the smaller tumors, but significantly lower in the larger tumors (4.6 ± 1.0 torr and 1.7 torr; $p < 0.001$). With oxygen inhalation, pO_2 increased significantly in both the smaller (mean = 179.6 ± 16 torr; median = 177.4 torr) and the larger tumors (mean = 110.2 ± 13.6 torr; median = 70.1 torr). For all tumors, irradiation produced a significant growth delay compared with sham irradiated controls, but for small tumors oxygen inhalation had no additional effect. By contrast, for the larger tumors, oxygen inhalation produced enhanced growth delay (enhancement ratio = 2.4).

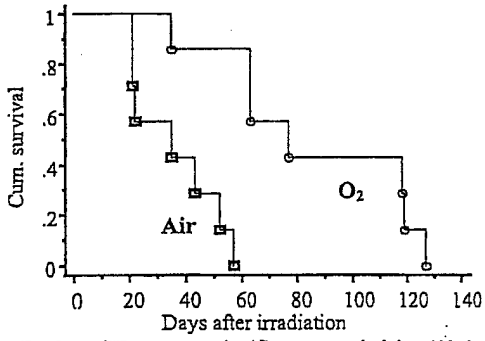

For large HI tumors a significant growth delay (50 days; $p < 0.01$) was observed when rats inhaled oxygen during irradiation. The Kaplan Meier survival plot indicates time to reach 3 x initial size (or earlier sacrifice, as needed).

Discussion: When rats breathed oxygen during irradiation, large HI tumors exhibited a significantly longer growth delay than those breathing air. For small tumors, no difference was observed. The differential behavior may be attributed to the low baseline hypoxic fraction (< 10 torr) in small tumors (20%) as a target for oxygen inhalation. Meanwhile, hypoxic fraction in the larger tumors dropped significantly from a mean baseline value 80% to a final value 21% after 40 min oxygen breathing ($p < 0.001$). These data suggest that the ability to detect modulation of tumor pO_2, in particular, the residual hypoxic fraction, with respect to an intervention, could have prognostic value for improving the efficacy of radiotherapy. These results further demonstrate the value of *FREDOM* to assess *in vivo* dynamic changes in regional pO_2 as a prognostic tool.

References:

1. Hunjan, S., Zhao, D., Constantinescu, A., Hahn, E. W., Antich, P. P., and Mason, R. P. *Int. J. Radiat. Oncol. Biol. Phys.* 49, 1097-1108, 2001.

2. Zhao, D., Constantinescu, A., Hahn, E. W., and Mason, R. P. *Radiat. Res.* 156, 510-520, 2001.

Acknowledgment: Supported by DOD Prostate Cancer Initiative (DAMD 170110108) and NCI RO1 79515.

INTERNATIONAL SOCIETY FOR MAGNETIC RESONANCE IN MEDICINE

Tenth Scientific Meeting and Exhibition

18 – 24 May 2002

Honolulu, Hawai'i, USA

Program

INTERNATIONAL SOCIETY FOR
ISMRM
MAGNETIC RESONANCE IN MEDICINE

Appendix E

Biographical Sketches

Provide the following information for the key personnel listed on page 1 of the Detailed Cost Estimate form (see Appendix F) for the initial budget period.

NAME	POSITION TITLE
DAWEN ZHAO	INSTRUCTOR

EDUCATION/TRAINING (Begin with baccalaureate or other initial professional education, such as nursing, and include postdoctoral training.)

INSTITUTION AND LOCATION	DEGREE (IF APPLICABLE)	YEAR(S)	FIELD OF STUDY
Dalian Medical University, Dalian, China	M.D.	1986-1991	Clinical Medicine
University of Tsukuba, Tsukuba, Japan	Ph.D.	1994-1998	Tumor Morpho-logy; MRI
Dept. Neurosurgery, University of Tsukuba, Tsukuba, Japan	Post-doc	1998-1999	Tumor Biology
Dept. Radiology, UT-Southwestern Medical Center, Dallas TX	Post-doc	1999-2001	NMR

RESEARCH AND PROFESSIONAL EXPERIENCE: Concluding with present position, list, in chronological order, previous employment, experience, and honors. Include present membership on any Federal Government public advisory committee. List, in chronological order, the titles, all authors, and complete references to all publications during the past 3 years and representative earlier publications pertinent to this application. PAGE LIMITATIONS APPLY. DO NOT EXCEED THREE PAGES FOR THE ENTIRE BIOGRAPHICAL SKETCH PER INVESTIGATOR.

2001- Faculty Research Instructor: Department of Radiology, UT Southwestern Medical Center, Dallas
2002- Faculty, Graduate School Program of Advanced Radiological Sciences, UT Southwestern

Prizes:
Postdoctoral fellow stipend, 8th International Society Magnetic Resonace in Medicine, Denver (Apr 2000)
Junior Investigator Award, 11th Tumor Physiology and Cancer Treatment Conference, Banff (Oct 2000)
Postdoctoral fellow Travel Award, 48th Radiation Research Society, San Juan (Apr 2001)

Membership of Professional Societies:
International Society of Magnetic Resonance in Medicine

Publications:

1. "Expression of p27kip1 and Ki-67 in pituitary adenoma: an investigation of marker of adenoma invasiveness" **Zhao, D.**, Tomono, Y., and Nose, T. *Acta Neurochir (Wien)* 141, 187-192, 1999.
2. "Copper/zinc superoxide dismutase, nuclear DNA content, and progression in human gliomas" Yoshii, Y., Saito, A., **Zhao, D.**, Nose, T. *J. Neuro. Oncol.* 42(2): 103-108, 1999.
3. "Immunohistochemical and ultrastructural study of clinically nonfunctioning pituitary adenomas" **Zhao, D.**, Tomono, Y., Tsuboi, K., Nose, T. *Neuro. Med. Chir.* 40, 453-57, 2000.
4. "Tumor Oximetry: an enhanced dynamic mapping procedure using ^{19}F echo planar MRI" Hunjan, S., **Zhao, D.**, Constantinescu, A., Hahn, E. W., Antich, P. P., and Mason, R. P. *Int. J. Radiat. Oncol. Biol. Phys.* 49, 1097-1108, 2001.
5. "Prognostic radiology: quantitative assessment of tumor oxygen dynamics by MRI" **Zhao, D.**, Constantinescu, A., Jiang, L., Hahn, E. W., and Mason, R. P. *Am. J. Clin. Oncol.* 24, 462-66, 2001.
6. "Tumor oxygen dynamics with respect to growth and respiratory challenge: investigation of the Dunning prostate R3327-HI tumor" **Zhao, D.**, Constantinescu, A., Hahn, E. W., and Mason, R. P. *Radiat. Res.* 156, 510-20, 2001.
7. "Differential oxygen dynamics in the two Dunning prostate R3327 rat tumor sublines (MAT-Lu and HI) with respect to growth and respiratory challenge" **Zhao, D.**, Constantinescu, A., Hahn, E. W., and Mason, R. P. *Int. J. Radiat. Oncol. Biol. Phys.* in the press 2002.
8. "Interplay of tumor vascular oxygenation and tumor pO_2 observed using NIRS, oxygen electrode, and ^{19}F MR pO_2 Mapping" Kim, J. W., Song, Y., **Zhao, D.**, Constantinescu, A., Mason, R. P., Liu H. *J. Biomed. Optics.* Submitted 2002.
9. "Correlation of tumor oxygen dynamics with radiation response of the Dunning prostate R3327-HI tumors" **Zhao, D.**, Constantinescu, A., Hahn, E. W., and Mason, R. P. *Radiat. Res.* Submitted 2002.

Sections of Edited Books

1. "Interplay of tumor oxygenation and pO_2 in tumors using NIRS and Needle electrode" Kim, J. W., Song, Y., **Zhao, D.**, Constantinescu, A., Mason, R. P., Liu H. *SPIE*, 4250, 429-36, 2001.
2. "Tumor oximetry: comparison of ^{19}F MR EPI and electrodes" Mason, R. P., Hunjan, S., Constantinescu, A., Song, Y., **Zhao, D.**, Hahn, E. W., Antich, P. P., and Peschke P. Oxygen Transport to Tissue XXII. Proceedings of the 27th annual meeting of the International Society on Oxygen Transport to Tissue. (Dunn, J. F. and H. M. Swartz Eds.), Pabst Verlag, in the press 2002.
3. "Tumor oxygen dynamics: Comparison of ^{19}F MR EPI and Frequency Domain NIR Spectroscopy" Song, Y., Worden, K. L., Jiang, X., **Zhao, D.**, Constantinescu, A., Liu, H., and Mason, R. P. Oxygen Transport to Tissue XXII. Proceedings of the 27th annual meeting of the International Society on Oxygen Transport to Tissue. (Dunn, J. F. and H. M. Swartz Eds.), Pabst Verlag, in the press 2002.

Abstracts (Selected from 28 Published Conference Proceedings)

1. "Tumor oxygen dynamics with respect to growth and respiratory challenge by ^{19}F MR EPI" **Zhao, D.**, Constantinescu, A., Hahn, E. W., Mason, R. P. p623, 8th ISMRM, Denver, Apr 2000.
2. "A comparison of oxygen dynamics during respiratory challenge in two Dunning prostate tumor sublines having diverse Tpots" **Zhao, D.**, Hahn, E.W., Constantinescu, A., and Mason, R.P. 47th Radiat. Res. Soc., Albuquerque, Apr 2000.
3. "Tumor oximetry: an enhanced dynamic mapping procedure using ^{19}F echo planar MRI" **Zhao, D.**,

Hunjan, S., Constantinescu, A., Song, Y., Hahn, E.W. Antich, P.P. and Mason, R.P. 47th Radiat. Res. Soc., Albuquerque, Apr 2000.

4. "Differential oxygen dynamics among the Dunning prostate R3327 rat tumor sublines with respect to growth and respiratory challenge" **Zhao, D.**, Hahn, E.W., Constantinescu, A., and Mason, R.P. #7 p25, 11th International Conference of on Chemical Modifiers of Cancer Treatment, Banff, Canada, Oct. 2000.
5. "Diverse approaches to monitoring oxygen dynamics in rat breast and prostate tumors" **Zhao, D.**, Song, Y., Liu, H., Constantinescu, A., Hahn, E.W., and Mason, R.P. #19 p55, 11th International Conference on Chemical Modifiers of Cancer Treatment, Banff, Canada, Oct 2000.
6. Differential oxygen dynamics among diverse Dunning prostate R3327 rat tumor sublines with respect to growth and respiratory challenge" **Zhao, D.**, Constantinescu, A., Hahn, E.W., and Mason, R.P. II-24, Society for Basic Urological Research, Ft. Myers, Nov 2000.
7. "Tumor vascular oxygen dynamics by near-infrared spectroscopy" Liu, H., Song, Y., **Zhao, D.**, Constantinescu, A., and Mason, R. P. Proc. SPIE. 4250, Optical Tomography and Spectroscopy of Tissue IV [4250-75] Jan 2001.
8. "Prognostic Radiology: quantitative assessment of tumor oxygen dynamics by MRI" **Zhao, D.**, Constantinescu, A., Hahn, E.W., and Mason, R.P. Proceedings of Translational Research Program Workshop, RTOG semi annual meeting, Tampa, FL, p21, Feb 2001.
9. "Comparison of tumor blood flow and oxygenation in two diverse Dunning prostate tumor sublines" **Zhao, D.**, Jiang, L., Constantinescu, A., Hahn, E.W., and Mason, R.P. #2088 p388. 92th AACR. New Orleans, LA, Mar 2001.
10. "Insight into interdependent parameters of tumor blood flow and oxygenation" **Zhao, D.**, Jiang, L., Constantinescu, A., Hahn, E.W., and Mason, R.P. #3 MS10. 48th Radiat. Res. Soc. San Juan, Peurto Rico, Apr 2001.
11. "Measuring tumor oxygen dynamics predicts beneficial adjuvant intervention for radiotherapy in Dunning prostate R3327-HI tumors" **Zhao, D.**, Constantinescu, A., Chang, K., Gall, K., Hahn, E.W., and Mason, R.P. #265 P21. *48th Radiat. Res. Soc.* San Juan, Peurto Rico, Apr 2001.
12. "Prognostic Radiology: the value of *FREDOM*" **Zhao, D.**, Constantinescu, A., Jiang, L., Chang, K., Gall, K., Hahn, E.W., and Mason, R.P. *Proc. EPR Viable Systems 9th International Meeting*, #S-8, Dartmouth, NH, Sep 2001.
13. "In vivo MRI monitoring of prostate tumor vasculature and oxygen dynamics" **Zhao, D.**, Jiang, L., Constantinescu, A., Hahn, E.W., and Mason, R.P. *AACR New Discoveries in Prostate Cancer Biology and Treatment*, # B-56, Naples, FL, Dec 2001.
14. "In vivo MRI monitoring of tumor oxygen dynamics and correlation with histological findings" **Zhao, D.**, Ran, S., Constantinescu, A., Hahn, E.W., and Mason, R.P. *4th International Symposium on Anti-Angiogenic Agents*, Dallas, TX, Jan 2002.
15. "Comparison of hypoxia and microvascular density in the slow growing well differentiated H vs. the faster growing anaplastic AT1 Dunning prostate R3327 rat tumor" **Zhao, D.**, Hahn, E.W., Constantinescu, A., Ran, S., and Mason, R.P. *49th Radiat. Res. Soc.* Reno, NV, Apr 2002.
16. "Measurement of tumor oxygen dynamics correctly predicts beneficial adjuvant intervention for radiotherapy in Dunning prostate R3327-HI tumors" **Zhao, D.**, Constantinescu, A., Chang, K., Gall, K., Hahn, E.W., and Mason, R.P. *10th ISMRM*, Honolulu, Hawaii, May 2002.
17. "Comparison of BOLD and Gd-DTPA contrast enhanced MRI for the assessment of the two prostate tumor sublines exhibits different vascular development" Jiang, L., **Zhao, D.**, Constantinescu, A., Hahn, E.W., and Mason, R.P. *10th ISMRM*, Honolulu, Hawaii, May 2002.